

CARMI: A Cache-Aware Learned Index with a Cost-based Construction Algorithm

Jiaoyi Zhang
Tsinghua University
Beijing, China

jy-zhang20@mails.tsinghua.edu.cn

Yihan Gao
Tsinghua University
Beijing, China

gaoyihan@mail.tsinghua.edu.cn

ABSTRACT

Learned indexes, which use machine learning models to replace traditional index structures, have shown promising results in recent studies. However, existing learned indexes exhibit a performance gap between synthetic and real-world datasets, making them far from practical indexes.

In this paper, we identify that ignoring the importance of data partitioning during model training is the main reason for this problem. Thus, we explicitly apply data partitioning to index construction and propose a new efficient and updatable cache-aware RMI framework, called CARMI. Specifically, we introduce entropy as a metric to quantify and characterize the effectiveness of data partitioning of tree nodes in learned indexes and propose a novel cost model, laying a new theoretical foundation for future research. Then, based on our novel cost model, CARMI can automatically determine tree structures and model types under various datasets and workloads by a hybrid construction algorithm without any manual tuning. Furthermore, since memory accesses limit the performance of RMIs, a new cache-aware design is also applied in CARMI, which makes full use of the characteristics of the CPU cache to effectively reduce the number of memory accesses. Our experimental study shows that CARMI performs better than baselines, achieving an average of $2.2\times/1.9\times$ speedup compared to B+ Tree/ALEX, while using only about $0.77\times$ memory space of B+ Tree. On the SOSP platform, CARMI outperforms all baselines, with an average speedup of $1.2\times$ over the nearest competitor RMI, which has been carefully tuned for each dataset in advance.

PVLDB Reference Format:

Jiaoyi Zhang and Yihan Gao. CARMI: A Cache-Aware Learned Index with a Cost-based Construction Algorithm. PVLDB, 14(1): XXX-XXX, 2020. doi:XX.XX/XXX.XX

PVLDB Artifact Availability:

The source code, data, and/or other artifacts have been made available at http://vldb.org/pvldb/format_vol14.html.

1 INTRODUCTION

As an indispensable access method of database systems, indexes provide fast data accesses by avoiding expensive table scans. Traditional index structures are general-purpose, in the sense that they

organize data according to fixed rules without taking advantage of the characteristics of underlying data distribution. Recently, Kraska et al. [27] pioneered a line of research where indexes are constructed using machine learning models. Specifically, they proposed a structure called the Recursive Model Index (RMI). In RMI, index nodes themselves are ML models, and they are connected hierarchically. To perform a lookup, we traverse the tree-like structure using the ML model in each node to determine the child branch to continue. Upon arriving at a position in the data array (i.e., leaf nodes), we perform the “last-mile” search within a range to correct the model prediction error. [27] demonstrates that the RMI and learned indexes in general exhibit smaller memory consumption and superior search performance compared to B+ Trees.

Despite the promising results shown in the latest research [16, 18, 19, 25, 27, 38, 49], few real database systems choose to adopt learned indexes. An outstanding reason, as indicated in the SOSP benchmark paper [24], is that the performance of learned indexes (represented by the RMIs) drops significantly when moving from synthetic datasets to real-world datasets. The average latency of an index lookup is $2.92\times$ larger on real-world datasets than that on the same-sized synthetic ones, as shown in [24].

We argue that the main reason behind such a performance gap lies in the fact that existing RMI designs overlook the importance of data partitioning during model training. Many current RMIs, including the original proposal [27], typically emphasize on the “model-fitting” aspect during index construction. Since the fanout and depth of the index are predetermined (and manually tuned), each leaf node is assigned a corresponding subset of the data and tries to train a model to fit the cumulative distribution function (CDF) of the assigned data as accurately as possible.

The consequence of such a rigid data partitioning strategy contributes to the large performance gap between synthetic and real-world datasets for RMIs. For synthetic datasets, the local data distribution at each leaf node is relatively “smooth” so that the expected prediction error is small, leading to a fast last-mile search. Real-world datasets, however, are much “bumpier”, and the degree of “bumpiness” varies across data ranges. Such irregularity in data distribution makes it difficult for simple models (e.g., linear regression) to achieve accurate predictions under predetermined or manually-tuned data partitions. Larger prediction errors require more memory accesses to correct and, therefore, hurt the index performance. Prior work such as [16, 19, 53] has attempted to automate partitioning during index construction. Their approaches, however, are heuristic-based and only work on a fixed model type, i.e., linear model.

In this paper, we propose to address the issue by explicitly incorporating data partitioning into the RMI construction process. First,

This work is licensed under the Creative Commons BY-NC-ND 4.0 International License. Visit <https://creativecommons.org/licenses/by-nc-nd/4.0/> to view a copy of this license. For any use beyond those covered by this license, obtain permission by emailing info@vldb.org. Copyright is held by the owner/author(s). Publication rights licensed to the VLDB Endowment.

Proceedings of the VLDB Endowment, Vol. 14, No. 1 ISSN 2150-8097.
doi:XX.XX/XXX.XX

we propose a new cost model that considers the data partitioning aspect for RMI training. The effectiveness of data partitioning is quantified using the entropy [21] over the number of data points in each partition. The intuition is that larger entropy indicates smaller partition sizes and a more even size distribution. Smaller partitions are preferable because they facilitate leaf-node training and produce more accurate models, especially on non-linear datasets. In addition, smaller child partitions flatten the hierarchical structure of RMI, and thus reduce cache misses. Meanwhile, more even child partitions lead to a more balanced tree structure.

Based on the new cost model, we formalize the index construction problem as an optimization problem and solve it using an algorithm combining the greedy and the dynamic programming approaches. Unlike CDFShop [38], where the node types for each layer are determined ahead of time, our algorithm selects the best model and the best partition fanout for each node automatically at construction time without the need for recompilation.

Finally, since memory accesses dominate the lookup performance for RMIs [36], we design the memory layout for each node in a cache-aware manner. Specifically, we require the size for every node with a model to be exactly the cacheline size (i.e., 64 bytes) so that each node visit (or model inference) incurs at most one cache miss. For leaf nodes containing data points across multiple cache-lines, we adopt a two-level B+ Tree design, consisting of a 64-byte root and multiple 256-byte data blocks. Such a cache-aware layout can effectively reduce the number of memory accesses during the last-mile search as in existing solutions [16, 25, 27, 38], especially on real-world datasets, with only a small space overhead. In addition, fixed-sized nodes facilitate memory prefetching where memory accesses are parallelized to further reduce the access latency.

We present our novel Cache-Aware RMI framework, called CARMi, that implements the new ideas introduced above with six example tree node (model) types. Our experimental study shows that CARMi outperforms all baselines on both our microbenchmark and SOSD benchmark. In our microbenchmark, CARMi achieves an average speedup of 2.2× (up to 4.2×) and 1.9× (up to 7.2×) compared to B+ Tree and ALEX, respectively, while only using about 0.77× memory space of B+ Tree. On the SOSD benchmark, CARMi achieves an average speedup of 2.5× (up to 3.0×)/1.5× (up to 2.3×) compared to B+ Tree/ALEX, respectively. Compared to its closest competitor RMI, which has been carefully tuned for each dataset in advance, CARMi is still 1.2× faster on average (up to 1.5×).

We make the following contributions:

- We identify that the inflexibility of data partitioning for learned indexes is one of the key reasons why there is a large performance gap when applying them to synthetic and real-world datasets.
- We propose a new cost model for RMI training, which uses entropy across partition sizes to measure the effect of data partitioning on index performance.
- We formalize the index construction problem as an optimization problem, and propose an algorithm to solve it efficiently and automatically.
- We propose CARMi, a novel RMI framework implementing the new cost model and automatic node selection algorithm. CARMi also uses a new memory layout that is more cache-friendly, especially for the last-mile search.

- We conduct a series of experiments to demonstrate the superior performance and robustness of our framework.

The remainder of this paper is outlined as follows: In Section 2, we review the RMI framework and discuss the two ways of viewing RMI: model fitting vs. data partitioning. In Section 3, we derive a cost model for the entire index structure, and introduce entropy as a metric for characterizing the node performance. Section 4 discusses the cost-based hybrid index construction algorithm, which is used to choose different node settings flexibly to construct the optimal index structure during runtime. In Section 5, we explain the cache-aware designs of CARMi, including the new memory layout and a prefetching mechanism. The experimental setup and results are shown in Section 6. We discuss the possible extension directions and future works in Section 7. Finally, we discuss related work in Section 8 and conclude in Section 9. Some implementation details, experimental settings and proof of theorem can be found in the appendix.

2 MOTIVATION AND CARMi

2.1 RMI and Data Partitioning

Figure 1 shows the structure of the Recursive Model Index (RMI), an ML-based index framework. Each inner node in the RMI represents an order-preserving regression model: the model $f : k \rightarrow idx$ takes a key k as input, and outputs an integer $idx \in \{1, 2, \dots, c\}$, where c is the number of child nodes of this inner node. The order-preserving property guarantees $k_1 \leq k_2 \Rightarrow f(k_1) \leq f(k_2)$ so that an RMI can answer range queries correctly. At the bottom layer, leaf nodes are trained using linear models to fit the underlying data points. Searching the RMI given k proceeds as follows: starting from the root, we evaluate the model to determine which child node to visit for the next step. This process is repeated until a leaf node is reached. Finally, we perform a binary search (bounded by the maximum error) to retrieve the matching records.

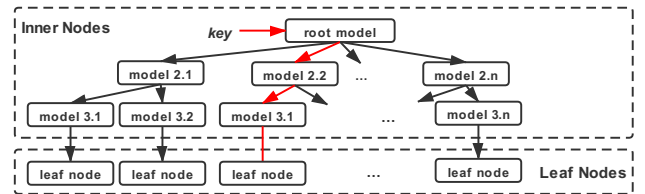


Figure 1: Learned Index

Existing RMI designs [16, 18, 19, 25, 27, 38, 49] view the index construction problem from the perspective of model fitting. In this view, models are trained to minimize a loss function (e.g., squared loss function) to best fit the CDF of a given dataset. Specifically, the root model targets at fitting the CDF of the entire dataset, while the leaf-node models try to fit their local distributions. Under such a problem setting, however, the index fanout and depth are typically predetermined before model training, and thus wasting opportunities to improve model accuracies through a more flexible data partitioning.

Approaching RMI construction via a “model-fitting” view can lead to a significant performance drop when shifting from synthetic datasets to real-world datasets. Because real-world datasets are often non-smooth and non-linear, as shown in Section 6.3, simple

models such as linear regression are not able to fit well in certain CDF ranges if the partitioning is too coarse-grained. Inaccurate predictions from the models then require additional procedures such as large range scans to finish the “last-mile” search. These large-range searches span many cachelines and require multiple memory accesses, resulting in performance degradation.

In this paper, we propose to look at RMI construction from a “data-partitioning” view, where the models aim to partition a given dataset more evenly into smaller chunks to form a flatter and more balanced tree. Moreover, larger fanouts (i.e., more child partitions) of the upper-level models are preferable in terms of the overall prediction accuracy because lower-level nodes now can work on smaller local datasets to reduce their maximum model prediction errors. The trade-off for more partitions, however, is the space overhead due to more nodes and the performance hit due to potentially more complex models. Therefore, we include the effectiveness of data partitioning in our new cost model along with search time and space, and develop an algorithm to train an RMI automatically using an objective function derived from the cost model.

To quantify the effectiveness of data partitioning, we propose to use entropy, an information-theoretic metric [21]. Suppose an inner node M distributes a total of n data points into c different child nodes¹, then the entropy $H(M)$ is defined as: $H(M) = -\sum_{i=1}^c p_i \log_2 p_i$, where $p_i = \frac{n_i}{n}$ and n_i is the number of data points allocated to the i -th child node. As mentioned in the introduction, larger entropies mean that datasets are divided more evenly into smaller subsets, which is more desirable as discussed above. Further, the entropy also helps establish the notion of local node efficiency, as described in Section 3.3.1, which combines the time and space cost of a single node and its dataset partitioning utility into a single metric. With this metric, we can effectively compare models locally without global information, thus speeding up index construction.

2.2 Overview of CARMi

In this paper, we extend the RMI framework and propose a refined general RMI framework that can automatically build suitable and updatable indexes for given datasets, called Cache-Aware RMI (CARMi). CARMi retains RMI’s core idea of replacing traditional indexes with ML models and has similar procedures for querying data points, but differs in specific designs. Specifically, in our new memory layout (§ 5), all tree nodes are limited to 64 bytes and stored in a single array. Then, according to the independent characterization of each tree node (§ 3), CARMi can use different nodes to handle different sub-datasets and link them into an index tree.

Nodes in CARMi are explicitly classified into two categories: inner nodes and leaf nodes. Inner nodes are intermediate bridges between root and leaf nodes, using models to determine the next branch. Leaf nodes are similar in concept to leaf nodes of B+ Tree, but they only store data points conceptually by storing pointers to data blocks containing actual data points.

For a given dataset, CARMi uses a hybrid construction algorithm (§ 4) to solve the index construction problem, whose optimization objective is to minimize the weighted sum of time and space costs

(§ 3). With this algorithm, CARMi can automatically construct indexes with good performance at runtime.

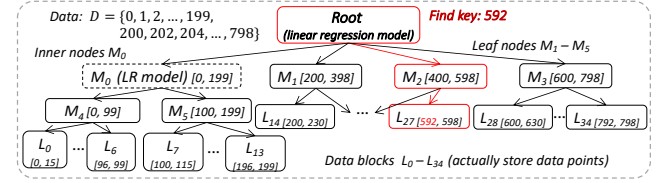


Figure 2: A Simple Example of CARMi

Then, we illustrate the design of CARMi via a concrete example:

EXAMPLE 1. Consider a dataset in which there are 500 data points $D = \{0, 1, \dots, 199, 200, 202, 204, \dots, 798\}$. Then CARMi can be a four-layer structure, as shown in Figure 2. The top layer is the root node with a linear regression (LR) model ($idx = \lfloor 0.005 \times key \rfloor$), which determines the index of the next node for each given key. The first 200 data points are managed by an LR inner node and its two child leaf nodes. The remaining 300 data points are directly managed by 3 leaf nodes ($M_1 - M_3$). Each leaf node is linked to 7 data blocks at the bottom and uses them to store data points.

Suppose that we need to access the record with key value 592. We first access the root node and use its model to calculate the index of the next node ($idx = \lfloor 0.005 \times 592 \rfloor = 2$). After obtaining the content of M_2 , we use its strategy to get the index of the data block (L_{27}), and finally, search for the key value 592 within L_{27} . Since the root node is frequently accessed, we assume that it is always in the cache memory. Therefore, for this example, we only need two random memory accesses: the leaf node M_2 and the data block L_{27} , respectively.

3 COST MODEL OF CARMi

In this section, we describe the new cost model of CARMi and its application in the index construction problem in detail. Specifically, to quantify the performance of tree nodes in a standalone fashion and lay a solid foundation for index construction, we first characterize each tree node from three dimensions: time cost, space cost, and entropy, and use them as building blocks to derive a cost model for the entire index structure. Since the analysis is performed from a generic perspective, the CARMi framework can accommodate any new types of tree nodes as long as they can be represented accordingly. Then, we use the cost model as an optimization objective to find the most suitable node design and tree structure at runtime. Some example tree node designs are briefly described in this paper, together with their performance characterization. These designs are all included in our open-source implementation of CARMi [1], and used in our experimental study in Section 6.

The rest of the section is organized as follows. We analyze the inner/leaf nodes from three perspectives in Section 3.1 and 3.2, respectively. The cost model of the entire index and the formal formulation of the index construction problem is described in Section 3.3. Finally, in Section 3.4, we briefly talk about a few specific tree node designs that we have implemented.

3.1 Inner Nodes

The main functionality of inner nodes is to determine which branch to go through, so that we can quickly map a given key to its corresponding leaf node. In the following, we discuss three separate

¹Note that the number of child nodes for an inner node is part of the model configurations, and we need to determine its optimal value when constructing the index.

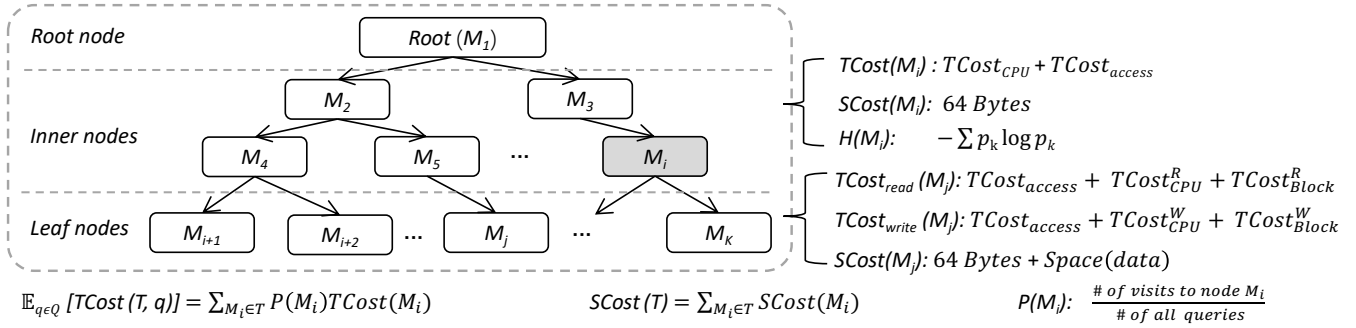


Figure 3: Cost Model of CARMi

dimensions for characterizing inner nodes: the time required for predicting the next branch, the space cost of the node, and the degree of uniformity of data points partitioning.

3.1.1 Time. The time cost of an inner node includes two parts: the access time and the computation time, denoted as $TCost_{access}$ and $TCost_{CPU}$, respectively. $TCost_{access}$ refers to the time to read the node content, which is equal to the latency of the main memory due to our cache-aware design in Section 5. $TCost_{CPU}$ is the time required for a model to compute the index of the next node, which only depends on the model type. Then, the total time required for an inner node M to predict the next branch is: $TCost(M) = TCost_{CPU} + TCost_{access}$.

3.1.2 Space. The space cost of an inner node M is the total amount of space in bytes, which is denoted as $SCost(M)$.

3.1.3 Entropy. We use the entropy metric to characterize the ability of an inner node to partition a dataset evenly. The entropy of an inner node M is: $H(M) = -\sum_{i=1}^c p_i \log_2 p_i$ (details in Section 2.1).

3.1.4 Root Node. In CARMi, the root node is handled differently compared to inner nodes: since the root node is always accessed during lookup procedures, we can assume that it is always available in the cache memory. Because of this, $TCost_{access}$ of the root node is equal to the latency of cache memory.

3.2 Leaf Nodes

Leaf nodes are used to manage the actual data points and can also be characterized in terms of time and space cost. The third dimension is the capacity for storing data points (i.e., how many data points can be stored in the leaf node).

In CARMi, we design a new type of leaf node similar to a two-level B+ tree node. Its root is 64 bytes and contains pointers to multiple 256-byte data blocks that store data points. Then, three dimensions of leaf nodes are described as follows.

3.2.1 Time. For leaf nodes, the time cost of two specific operations is analyzed: insert a new data point and lookup a data point².

Similar to inner nodes, the time to access the node ($TCost_{access}$) is equal to the main memory access latency. Due to the new leaf node, finding a data point requires first finding the index of the data block, and then locating the data point within the block. Their time costs are denoted as $TCost_{CPU}^R$ and $TCost_{Block}^R$, respectively.

²Deletion and update operations are not discussed since they are similar to the read access operations (we adopt a lazy deletion approach).

As for the insert operation, the content of both leaf node and data blocks might need to be changed accordingly. To reflect this, the time cost is denoted using a different superscript ($TCost_{CPU}^W$ and $TCost_{Block}^W$).

Overall, the time cost of a leaf node is modeled as:

$$\begin{aligned}
 TCost_{read}(M) &= TCost_{access} + TCost_{CPU}^R + TCost_{Block}^R \\
 TCost_{write}(M) &= TCost_{access} + TCost_{CPU}^W + TCost_{Block}^W
 \end{aligned} \tag{1}$$

3.2.2 Space. The space cost of a leaf node M , consists of the bytes of metadata and data blocks. Then the total space cost is:

$$SCost(M) = SCost_{leaf} + Space(data) \tag{2}$$

where $SCost_{leaf}$ is 64 bytes, and $Space(data)$ is the total amount of space occupied by the data blocks.

3.2.3 Capacity of Leaf Nodes. The capacity of leaf nodes refers to the total number of data points stored in a leaf node, and it depends on both the total amount of space allocated for data points as well as the way these data points are arranged. For example, if we need to make room for subsequently inserted data points to reduce the latency of the insert operation, then the capacity of the leaf node will be reduced accordingly.

3.3 The Optimization Problem

Based on the above analysis, we can define a cost model for the entire index structure. The time cost of queries can be estimated by utilizing the above analysis results: For any query q and index structure T , let the traversal path of q in T be $M_1(\text{root}) \rightarrow M_2 \rightarrow \dots \rightarrow M_k(\text{leaf})$, then the time cost of q can be approximated as:

$$TCost(T, q) = \sum_{i=1}^k TCost(M_i) \tag{3}$$

The space cost of the index structure is simply the sum of the space cost of all inner nodes and leaf nodes:

$$SCost(T) = \sum_{M_i \in T} SCost(M_i) \tag{4}$$

Now we can formalize the problem of index construction as an optimization problem: We would like to find the optimal index structure that minimizes the average time cost of each data lookup operation, under a certain space cost budget. Here the average time cost is evaluated with respect to a fixed query workload known in advance. The query workload can be constructed using recent history queries from users. In most cases, recent history queries

will faithfully reflect the characteristics of queries we expect to see in the future. If there are no history queries available, then we can use a uniform access workload instead, in which each data point is accessed exactly once.

The problem of finding an optimal tree structure is formulated as follows:

PROBLEM 1. *Let $Q = \{q_1, \dots, q_m\}$ be a collection of queries, and $D = \{d_1, \dots, d_n\}$ be the collection of keys to be maintained in the index structure. Find the optimal index tree structure T such that $\mathbb{E}_{q \in Q}[TCost(T, q)]$ is minimized, under the constraint that the total space cost of T does not exceed a fixed budget B : $SCost(T) \leq B$.*

Problem 1 is a constrained optimization problem, and a widely used technique for solving such problems is to use the Lagrange multiplier method [10] to transform it into an unconstrained problem. By utilizing this technique, Problem 1 can be transformed into a roughly equivalent form with a linear combination of time and space cost as objective, which is relatively easier to optimize:

PROBLEM 2. *Let $Q = \{q_1, \dots, q_m\}$ be a collection of queries, $D = \{d_1, \dots, d_n\}$ be the collection of keys to be maintained in the index structure, and λ be a positive constant parameter. Find the optimal index tree structure T such that $\mathbb{E}_{q \in Q}[TCost(T, q)] + \lambda SCost(T)$ is minimized.*

Problem 2 suggests that we ultimately want to minimize a weighted sum of time and space cost of the index, and we will describe an algorithm for solving it in Section 4.

Let $P(M_i)$ be the fraction of history queries passing through a tree node M_i . Then the expression $\mathbb{E}_{q \in Q}[TCost(T, q)]$ can be rearranged into an alternative form, which is sometimes more convenient:

$$\mathbb{E}_{q \in Q}[TCost(T, q)] = \sum_{M_i \in T} P(M_i) TCost(M_i) \quad (5)$$

Finally, a summarization of CARMi cost model can be found in Figure 3 for fast reference.

3.3.1 Theoretical Analysis. In the following analysis, we assume the history queries to be a uniform access of the data points for simplicity, in such a case the value of $P(M_i)$ is the same as the total fraction of data points in the subtree of M_i . With this assumption, the following theorem establishes a connection between $\sum_i P(M_i)H(M_i)$ and the total number of data points n .

THEOREM 3.1. *Let $T = \{M_1, \dots, M_K\}$ be an index structure with K nodes in total. $P(M_i)$ represents the ratio of data points in node M_i relative to the total number n . Then we have: $\sum_{i=1}^K P(M_i)H(M_i) = \log_2 n$, where for leaf nodes, $H(M_i)$ is defined as $\log_2(Capacity(M_i))$ and $Capacity(M_i)$ is the capacity of leaf nodes (§ 3.2.3).*

The proof of this theorem can be found in the appendix. Essentially, Theorem 3.1 states that the weighted sum of the entropy of all tree nodes is always a constant value. In other words, entropy characterizes the ‘‘contribution’’ of each tree node to the index structure: the higher entropy each tree node contributes, the less overall number of tree nodes we need in the index structure.

It is also of interest to compare Theorem 3.1 with the optimization objective of Problem 2. We can rewrite the objective using

Equation 5:

$$\text{Objective} = \sum_{i=1}^K [P(M_i) TCost(M_i) + \lambda SCost(M_i)]$$

Comparing with Theorem 3.1, we see that intuitively each tree node M contributes $P(M)H(M)$ entropy-wise to the index structure while incurring $P(M)TCost(M) + \lambda SCost(M)$ cost to the overall objective. Thus the ratio of these two terms can be used to quantify the local efficiency of node M :

$$\text{cost-ratio}(M) = \frac{P(M)TCost(M) + \lambda(SCost(M))}{P(M)H(M)} \quad (6)$$

Generally, we want to minimize the cost-ratio of all tree nodes, especially the ones with a large value of $P(M)H(M)$. For example, if all tree nodes have a cost-ratio less than c , then the optimization objective would be bounded by $c \log_2 n$.

Table 1: The Mechanism of Various Types of Nodes

Node	Mechanism
LR	Use a LR model to determine the corresponding branch
P. LR	Similar to LR nodes, but use a piecewise linear regression model instead
Hist	Determine the branch through a histogram lookup table
BS	Use binary search to determine the branch, similar to B+ Tree node
CF Array	A two-layer cache-friendly structure similar to a B+ Tree
Ext. Array	Only store meta data, and data points are stored in an external location

3.4 Specific Implementation

We have implemented four types of inner nodes and two types of leaf nodes in CARMi. For inner nodes, they use either linear regression, piecewise linear regression, binary search or histogram models to predict the next branch. For leaf nodes, we implemented two different structures: cache-friendly array (CF array) and external array. CF array leaf nodes store data points compactly in the data blocks in a sequential manner, and leaf node itself stores the minimum key values of data blocks. External array leaf nodes are used for primary index structures, where the original data points are already sorted according to the key value and stored in an external location. In such a case, we only need to store pointers to external locations in the leaf node.

Note that the choice of inner/leaf nodes can be flexibly determined at runtime and do not need to agree on a single one throughout the tree structure. Table 1 summarizes the mechanism and characteristics of each tree node type. The specific implementation details can be found in the appendix.

3.4.1 Empirical Performance. In order to evaluate the empirical performance of tree nodes, we have implemented a profiler program to evaluate the CPU computation time required for each node to obtain the position of the next branch and the time to obtain their contents from memory. Table 2 shows the empirical performance

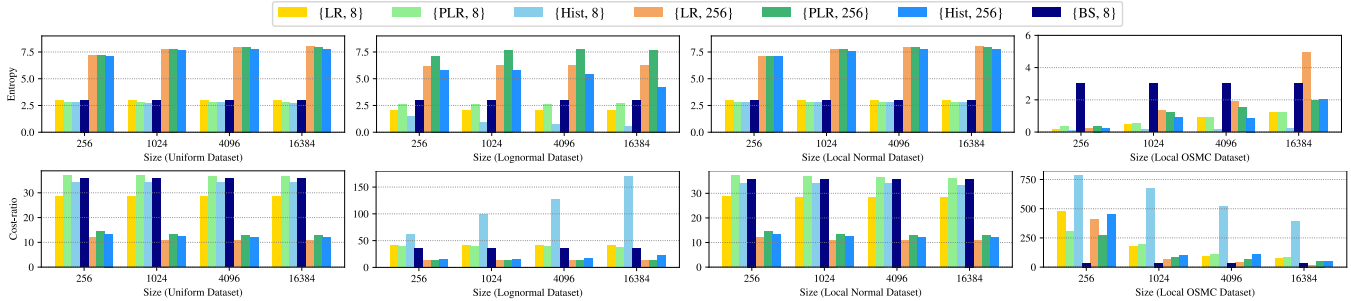


Figure 4: Entropy and cost-ratio, where each case is a node setting consisting of node type and number of children.

of these node types based on our evaluation on an Ubuntu platform equipped with an AMD Ryzen 3700X 8-Core Processor and 32GB RAM.

Table 2: The Empirical Values of Nodes in CARMi

Type	Node	Space (Bytes)	Time (ns)	
			Access	CPU
Root	LR	20	8.29	3.25
	P. LR	76	11.24	18.38
Inner	LR			5.2
	P. LR	64	80.09	22.8
	Hist			14.1
	BS			27.3
Leaf	CF (leaf node)	64	80.09	25.4
	CF (data block)	256	90.09	53.8
	Ext. Array	64	80.09	117.1–328.3

We also evaluate the entropy and the cost-ratio of inner nodes on three synthetic datasets and one real-world dataset in Figure 4. Detailed descriptions of the datasets can be found in Section 6.1. We provide the results of two different cases: (a) on two full synthetic datasets: uniform and lognormal datasets, (b) on random consecutive n data points in normal and OSMC datasets to show the results of local distributions. The number of key values in each case is 256, 1024, 4096, 16384, and the number of child nodes is 8 and 256, respectively.

1) Analysis of Root Nodes. Since the root node is frequently accessed and always in the cache memory, we do not need to limit the size of the root node, and can choose the node with a larger entropy to improve the overall performance. The LR node only needs a small amount of time (3.25 ns) to calculate the position of the next branch, while the P. LR node needs 18.38 ns.

2) Analysis of Inner Nodes. Due to the cache-aware design, the space cost of inner nodes is the same, but the time cost is different. The LR node enjoys the minimum CPU time cost of 5.2 ns, while other nodes need more time to get the position of the next branch. Note that even for the most costly BS nodes (27.3 ns), the CPU computation time is still much less than the access time, confirming our earlier intuition that we should try to minimize the number of memory accesses.

The utility of inner nodes on different datasets can be effectively reflected by entropy, and can be combined with time/space cost to help flexibly determine the appropriate nodes during construction. As shown in Figure 4, LR nodes handle linear datasets well (e.g., uniform dataset, local normal dataset), obtaining the largest entropy

close to $\log_2 c$ and lowest cost-ratio. However, ML nodes cannot achieve good utility with the same number of children as BS nodes since the distribution of local OSMC dataset is highly non-linear. In this case, BS nodes that can maintain the entropy of $\log_2 c$ are most suitable. Overall, these results validate that the data partitioning view is valuable and that it makes sense to use different nodes to build indexes flexibly.

3) Analysis of Leaf Nodes. The time cost of these two leaf nodes suggests that they are suitable for different situations. Since LR models and binary searches are required to lookup data points, the time cost of external leaf nodes varies greatly (117.1–328.3 ns) depending on the capacity and data distribution. When search ranges are small, this node only takes 197.19 ns to find the exact location, and thus, it is more suitable for linear datasets (e.g., YCSB dataset). CF leaf nodes can be widely used on various datasets, since only two memory accesses are required to obtain data points regardless of data distributions.

4 INDEX CONSTRUCTION ALGORITHM

In Section 3.3, we have shown that the optimal index tree structure can be constructed by minimizing the weighted sum of the time and space cost of the index structure (see Problem 2). In this section, we describe an algorithm for solving it.

First, let us rearrange the optimization objective as follows:

$$\mathbb{E}_{q \in Q} [TCost(T, q)] + \lambda SCost(T) = TCost(root) + \lambda SCost(root) + \sum_{i=1}^c \left[\frac{|Q_{T_i}|}{|Q|} \mathbb{E}_{q \in Q_{T_i}} [TCost(T_i, q)] + \lambda SCost(T_i) \right] \quad (7)$$

where c represents the number of child nodes of the root node, T_i is the sub-index tree of the i -th child node, and Q_{T_i} is the collection of queries that access T_i . Note that the number of child nodes is chosen from an exponentially increasing sequence to reduce training time, such as the powers of 2.

As we can see, the terms inside the square brackets have a very similar form compared to the original objective. In other words, once the root node of this subtree is fixed, the original optimization problem can be broken down into several independent sub-problems of similar form, and each sub-problem can be solved independently. For each sub-problem, we have two different algorithms for solving it:

- **Node selection algorithm:** A greedy algorithm that only considers local information to construct nodes, which is used when the subtree manages a large dataset (e.g., the root node).

- **Dynamic programming (DP) algorithm:** This algorithm is guaranteed to find the optimal sub-structure but is slower, and we only use it when the sub-dataset is small.

These two algorithms are used in combination in our construction algorithm. Then, the overall workflow for constructing the index structure for a given dataset is:

- First, we choose a root node setting using the greedy node selection algorithm.
- Next, we use the setting obtained in the previous step to assign the dataset to the child nodes of the root, and then construct a sub-index tree over each assigned sub-dataset.
- Each child node chooses the appropriate algorithm to build the sub-index structure according to the size of sub-dataset.
- Finally, all the sub-structures are merged together and linked to the root node to form the complete index tree.

The rest of this section is organized as follows: The greedy node selection step is described in Section 4.1 and the DP algorithm is described in Section 4.2. We provide a simple example to illustrate our construction algorithm in Section 4.3.

4.1 Node Selection Algorithm

For nodes that manage a large fraction of the dataset, such as the root node, we hope to quickly select a suitable node design using only local information. Below, we develop a greedy node selection algorithm to find the locally optimal solution without considering the design of the lower-level nodes:

- For the current node, the node selection algorithm enumerates various possible node types and considers a number of choices for the number of child nodes. For each enumerated setting, we calculate the time cost, space cost and entropy of the node.
- Then, we calculate the cost ratio of each setting using Equation 6 in Section 3.3, and select the setting with the minimum cost ratio for the current node.
- Using the setting (model and child number) obtained in the previous step, we assign each data point to one of the child nodes of the current node.
- Finally, the sub-index tree of each child node is constructed recursively using either this algorithm or the dynamic programming algorithm in the next section.

The pseudocode of the greedy node selection algorithm is shown in Algorithm 1. Note that we are not directly using the space cost of the node itself for computing the cost-ratio, but rather the total space cost of the child nodes of node M . The reason behind such a design is that the original cost-ratio would always favor large number of child nodes (since the time/space cost of the node itself is fixed). This change allows the greedy algorithm to choose a more reasonable node setting.

4.2 Dynamic Programming Algorithm

As shown in Equation 7, the original optimization problem can be decomposed into similar sub-tasks once the root node is fixed. Based on this intuition, we can use a dynamic programming algorithm to solve this problem:

- **State:** The state of each step is the dataset handled by the current node, denoted as $D_{l,r}$, where l and r are the left and right index

Algorithm 1 The Greedy Node Selection Procedure

Input: keys $K[]$, access frequency $f[]$, query number m ;
Output: local optimal design M

- 1: $OptimalValue \leftarrow \infty$
- 2: $P \leftarrow \sum_{j=1}^{|f|} f_j/m$
- 3: **for** every inner node design M_i **do**
- 4: $K_1, \dots, K_{c_i} \leftarrow \text{Partition}(K, M_i)$
- 5: $ChildSCost \leftarrow c_i \times 64 \text{ bytes}$
- 6: $Cost \leftarrow TCost(M_i) + \lambda \times ChildSCost/P$
- 7: **for** $j = 1$ **to** c_i **do**
- 8: $p_j \leftarrow |K_j|/|K|$
- 9: **end for**
- 10: $H(M_i) \leftarrow -\sum_{j=1}^{c_i} p_j \log_2 p_j$
- 11: **if** $(Cost/H(M_i)) < OptimalValue$ **then**
- 12: $OptimalValue \leftarrow Cost/H(M_i)$
- 13: $M \leftarrow M_i$
- 14: **end if**
- 15: **end for**
- 16: **return** M

of the entire dataset. Let $Q_{l,r}$ be the collection of queries that access $D_{l,r}$, and $T_{l,r}$ be the sub-index tree for $D_{l,r}$. Then the corresponding entry $cost[l, r]$ in DP table is the value of the following expression:

$$cost[l, r] = \min_{T_{l,r}} \left\{ \frac{|Q_{l,r}|}{|Q|} \mathbb{E}_{q \in Q_{l,r}} [TCost(T_{l,r}, q)] + \lambda SCost(T_{l,r}) \right\} \quad (8)$$

- **State transition equation:** Let S be the collection of all possible settings for the root node of sub-index tree, including the type of the root node and the number of the child nodes. Then according to Equation 7 and 8, the state transition equation is:

$$cost[l, r] = \min_{(M,c) \in S} \left\{ \frac{|Q_{l,r}|}{|Q|} TCost(M) + \lambda SCost(M) + \sum_{j=1}^c cost[l_j, r_j] \right\}$$

where M and c are the node type and the number of child nodes (if the node is a leaf node, c is 0), respectively, l_j and r_j are the left and right index of the sub-dataset that belongs to the child node j . If the dataset is smaller than a certain threshold, then we only consider the leaf node settings in the state transition equation.

Specifically, given a sub-dataset $D_{l,r}$, we need to enumerate all its possible settings for the root node, and compute the cost of each setting separately. Then, the setting with minimum cost is selected to construct the current node, and the cost is stored to the entry $cost[l, r]$. For each setting, we first look up the time/space cost of the root node from our cost model, and use the sub-dataset $D_{l,r}$ to train the root node model M . Then, we use the trained model M to assign the dataset to c child nodes and obtain their cost via a memorized search approach: for each subtask of computing $cost[l_j, r_j]$, the algorithm first checks whether it has been solved before. Then according to the check result, it either returns the minimum cost directly from the DP table or recursively calls the process of the DP algorithm. When the number of data points in the subtree is less than a pre-specified threshold, the algorithm will directly construct a leaf node as the current node. Otherwise, the algorithm considers two cases (leaf nodes or subtrees with inner nodes) and

chooses the optimal design according to the transition equation. The pseudocode of the DP algorithm is shown in Algorithm 2.

Algorithm 2 DP Algorithm

Input: keys $K[]$, queries $Q[]$, left index l , right index r ;
Output: optimal structure $T_{l,r}$, $\frac{|Q_{l,r}|}{|Q|} \mathbb{E}_{q \in Q_{l,r}} [TCost(T_{l,r}, q)] + \lambda(SCost(T_{l,r}))$

```

1: if sub-problem  $(l, r)$  have been solved before then
2:   return  $(T_{l,r}, cost[l, r])$ 
3: end if
4: /*kLeafMaxCapacity must be larger than kLeafThreshold*/
5: if  $r - l + 1 \leq kLeafMaxCapacity$  then
6:   Construct a leaf node  $T_{l,r}$  from  $K[l, \dots, r]$  and  $Q[l, \dots, r]$ .
7:    $OptValue \leftarrow \frac{|Q_{l,r}|}{|Q|} \mathbb{E}_{q \in Q_{l,r}} [TCost(T_{l,r}, q)] + \lambda(SCost(T_{l,r}))$ 
8: end if
9: if  $r - l + 1 > kLeafThreshold$  then
10:  for every inner node design  $M$  do
11:     $(\{l_1, r_1\}, \dots, \{l_c, r_c\}) \leftarrow \text{Partition}(K[l, \dots, r], M)$ 
12:    for  $j = 1$  to  $c$  do
13:       $(T_{l_j, r_j}, cost[l_j, r_j]) \leftarrow \text{DP}(K, Q, l_j, r_j)$ 
14:    end for
15:     $RootCost \leftarrow \frac{|Q_{l,r}|}{|Q|} TCost(M) + \lambda(SCost(M))$ 
16:    if  $\sum_j cost[l_j, r_j] + RootCost < OptValue$  then
17:       $OptValue \leftarrow \sum_j cost[l_j, r_j] + RootCost$ 
18:      Construct an index structure  $\{T_{l_j, r_j}\}$  from  $T_j$  and  $M$ 
19:    end if
20:  end for
21: end if
22: return  $(T_{l,r}, OptValue)$ 

```

Although in principle, the dynamic programming algorithm can be used to construct the optimal index structure for the entire dataset, in practice, it is too slow to handle large datasets. Therefore, we only use it to solve sub-problem that are small enough.

4.3 A Simple Example

Here we use the same example as before to demonstrate the entire index construction process.

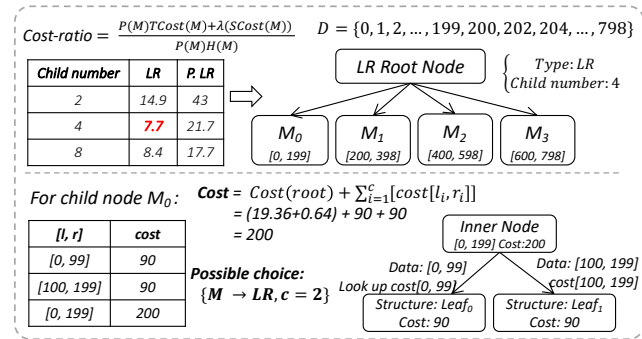


Figure 5: Construct the Root/Inner Node

EXAMPLE 2. We demonstrate our construction algorithm using the dataset $D = \{0, 1, \dots, 199, 200, 202, \dots, 798\}$ in Figure 5. First, we use

the greedy node selection algorithm to choose the setting of the root node. We consider two node types: LR and P.LR, and compute their cost ratios with 2, 4, and 8 child nodes, respectively. Among them, the LR root node with 4 child nodes has the minimum cost ratio of 7.7. Therefore, we use it to construct the root node and assign the dataset to the 4 child nodes according to the trained LR model.

We use sub-datasets to construct the optimal sub-trees for 4 child nodes according to the DP algorithm. We need to enumerate all possible settings for them. For example, for node M_0 with $D_{0,199}$, a possible setting is that the type is the LR inner node and the number of child nodes is 2. After looking up its cost of 20, we use the trained LR node to assign the dataset to the child nodes and obtain two smaller sub-datasets: $D_{0,99}$ and $D_{100,199}$. According to the state transition equation, the algorithm needs to compute the minimum cost for the two sub-datasets. Here we assume that their cost has already been computed previously, therefore, we only need to look up $cost[0, 99]$ and $cost[100, 199]$ in the DP table (both are 90). Then, we can get the overall cost of 200 by adding up all three costs. After enumerating each possible choice, we use the setting with the minimum cost to construct M_0 . Then, for $M_1 - M_3$, we repeat the above steps and select a leaf node as their root node. Finally, the optimal index structure can be obtained by linking these four subtrees with the root node.

5 CACHE-AWARE DESIGN

In this section, we describe the cache-aware design of CARMI with a new memory layout in detail, use some examples to explain the intuition and benefits of such a design, and also discuss the potential opportunities for using memory prefetching instructions to further speed up queries.

The rest of this section is organized as follows: Section 5.1 discusses the details of cache-aware design, and Section 5.2 describes our new memory layout and the basic lookup and insert operations. The use of memory prefetch will be discussed in Section 5.3.

5.1 Details of Cache-Aware Design

B+ Trees with tree nodes occupying exactly a cache line size can outperform standard binary search trees [47]. Specifically, each memory access always copies a fixed-size memory content (i.e., cache line size, usually 64 bytes), then indexes that utilize the cache and do not “waste” any data retrieved into cache memory can generally outperform standard data structure by a large margin.

In CARMI, we employ the same design decision as in B+ Tree and enforce all tree nodes to have a fixed size of 64 bytes. To understand the intuition behind such a design, we briefly analyze the performance bottleneck of the lookup procedure in RMI. For an index structure within the RMI framework (shown in Figure 1), the procedure for accessing a data point is as follows:

- We first access the content of the root node, and then use its model to choose a child node of the root.
- Subsequently, in each layer, we visit a node chosen by the node in the previous layer, and then use the model of this node to choose one of its child nodes. We repeat this step until we have reached a leaf node.

In the above procedure, for each tree node, we need at least one memory access to get its content before performing the model computation. For simple models (e.g., linear models), the computation

time is usually less than 20 ns, while a memory access takes about 70-100 ns if the node content is not cached. Therefore, the time required for memory access would actually take up most of the time we spent on data lookup. In other words, the performance bottleneck of RMI is memory access.

Based on the above analysis, we hope to minimize the number of memory accesses and fully utilize each access during data lookup. In CARMI, we achieve them from the following two aspects.

First, we enforce each node to have a size of exactly 64 bytes to align the cache line. This design allows the node to be fetched with only one memory access. Furthermore, the large node size allows it to store rich information, which helps to reduce the average tree depth, thus reducing the number of needed memory accesses.

To further reduce the number of memory accesses in the last mile, we design a new leaf node called Cache-Friendly array leaf node, which is conceptually similar to a two-layer B+ Tree node. The first layer is a 64-byte root that stores pointers to several 256-byte data blocks in the second layer and the minimum key values of each block. With such a design, we only need one memory access to obtain metadata to determine the next data block and narrow down the last-mile search range to 256 bytes, effectively reducing memory accesses on real-world datasets.

5.2 Memory Layout

For the memory layout of CARMI, we have two main arrays, *data* and *node*, to assist in implementing our cache-aware design. These two arrays are used to store data points and tree nodes, respectively, as shown in Figure 6, with details as follows:

- **Data array:** The *data* array is used to store data points in CARMI. It is a large array containing many small data blocks, each of which has a fixed size, represented by a parameter *kBlockSize* with a default value of 256. Data points are stored in these data blocks. In the *data* array, data blocks managed by the same leaf node are stored in adjacent locations.
- **Node array:** All tree nodes, including both inner and leaf nodes, are stored in the *node* array. Each tree node occupies a total of 64 bytes: the first byte is always the node type identifier, and the next three bytes are used to store the number of child nodes (the number of data blocks for leaf nodes). For inner nodes, the following 4 bytes represent the starting index of the child nodes in the *node* array. For leaf nodes, they store the starting index of data blocks in the *data* array instead. The remaining 56 bytes store additional information depending on the tree node type.

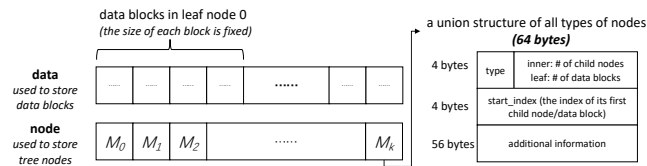


Figure 6: Memory Layout

With the help of the above two arrays, we can perform operations such as lookup and insert. The way we use them in lookup and insert operations is described below.

5.2.1 Lookup Operation. When accessing a data point, we first use the root node model to compute the index of the node in the next layer. Next, we access the tree node according to the index value and use its model to update the value of the index variable. This process is repeated iteratively until a leaf node is visited. Finally, we search within this leaf node to get the corresponding data record. The pseudocode of the data access process can be found in Algorithm 3.

Algorithm 3 Lookup

Input: *key*
Output: *data*

```

1:  $idx \leftarrow root.Predict(key)$ 
2: while true do
3:   if  $node[idx].type == inner\_node$  then
4:      $idx \leftarrow node[idx].Predict(key)$ 
5:   else
6:     /* access leaf node */
7:      $l \leftarrow node[idx].start\_index$ 
8:      $p \leftarrow node[idx].Predict(key)$ 
9:      $res \leftarrow SearchBlock(data[l + p], key)$ 
10:    return  $data[l + p].slots[res]$ 
11:   end if
12: end while

```

5.2.2 Insert Operation. The basic process of the insert operation is similar to the lookup operation. After finding the correct data block for insertion, we insert the data point into it. In addition, there are two mechanisms that can be initiated by the leaf node under certain situations:

- **Expand:** When a leaf node needs more space, it can initiate an expand operation to get more data blocks. We first collect all the data points stored in it, and then construct a new leaf node at a new location with more space, as shown in Figure 7. The new leaf node then replaces the original one to complete the process.
- **Split:** If we can no longer use a single leaf node to efficiently manage all the data points, it needs to be split. The leaf node will be replaced with a subtree consisting of a new inner node and several new leaf nodes, as shown in Figure 7. The number of leaf nodes in the subtree depends on the trained model of the new inner node.

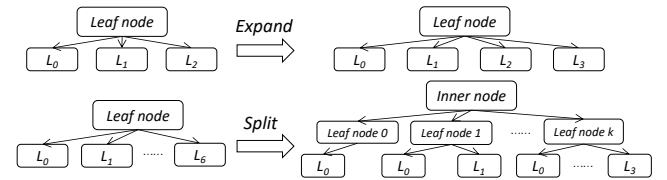


Figure 7: Expand and Split Mechanism

5.3 Prefetch

5.3.1 Prefetch Mechanism. In some cases, when the key value distribution in the dataset is very regular (e.g., uniform distribution), the index of the data block can be directly predicted from the input key value. In such cases, we can further reduce the data access latency by utilizing memory prefetching. More specifically, we add

an additional prefetch model to the root node to predict the data block where a given key value may be stored. Therefore, during the access process, the predicted data block is prefetched at the root node, which can be executed in parallel with other memory accesses in the normal process. If the prediction is correct, then the data block will be available in the cache when we need to access it. In this way, for datasets with regular data distribution, we can speed up the access to a certain extent. We demonstrate the prefetch mechanism via the following example:

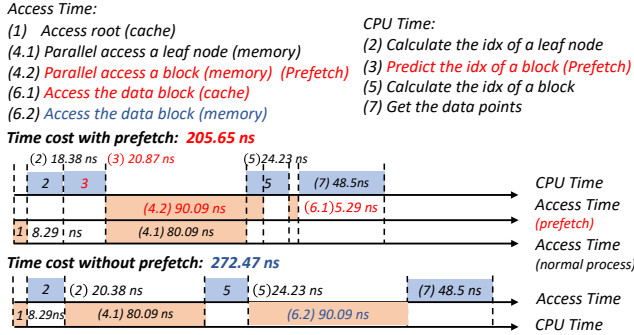


Figure 8: Memory Prefetch in CARMi

EXAMPLE 3. We use the same settings as in Example 1 to show the effect of prefetching. The time cost of accessing a data point in CARMi can be divided into two parts: CPU time and access time. In this example, we need to access: the root node (8.29 ns), the leaf node (80.09 ns), and the data block (90.09 ns). The CPU time consists of model calculations in the root node (20.38 ns), the leaf node (24.23 ns), and the search process (48.5 ns) in the data block. Note that the CPU calculations must wait until the corresponding cache/memory access is completed before it can be processed. Therefore, without prefetching, CPU calculations and access operations are performed alternately and do not overlap, which constitutes a total time cost of 272.47 ns.

To utilize the prefetch mechanism, we need to add an additional 28.87 ns of CPU time to predict the index of the data block that needs to be prefetched, so that we can then prefetch this data block in advance at the root node. The benefit of this prefetching step is that, when we actually need the data block later on in the process, it will be already in the cache and be retrieved very quickly, reducing the time cost of a memory access. In general, a lookup operation with prefetching only requires 205.65 ns in this example, which reduces the time by 67 ns compared to the situation without prefetching.

5.3.2 *Prefetch Support.* In order to support the prefetching design, we need to make a few changes to the construction algorithm: we need to add an additional model at the root node to predict the index of the data block, and we also want to store data points in data blocks according to the prefetch prediction model whenever possible.

This prefetch prediction model is used to predict the index of the data block corresponding to each key value during the lookup procedure, and we store data points in data blocks according to the model during the construction of the index structure whenever possible.

More specifically, we use a piecewise linear regression model as the prefetch prediction model. The prefetch prediction model

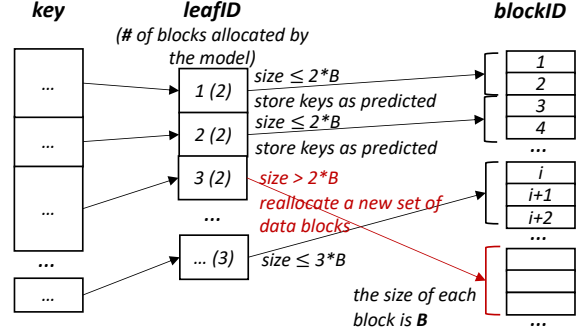


Figure 9: Prefetch Support

requires access to the raw output of the root model (leaf index before rounding down), and then use it as input to the piecewise linear model to compute a block index. Note that by the time we start to construct the prefetch prediction model, the root node has already been determined by the greedy node selection algorithm. Therefore, the unrounded leaf node index can be directly obtained from the root node.

In the piecewise linear regression model, we force the slope and intercept of each segment to be integers, so that within each segment, each leaf node is mapped to the same number of data blocks. For each leaf node, we first attempt to allocate its data blocks according to the prefetch prediction model, and check whether the current leaf node has enough capacity to store all assigned data points. If the leaf node has enough capacity, then we simply store the data points in these data blocks. Otherwise, we reallocate a new set of data blocks for the current leaf node at another irrelevant location. Figure 9 illustrates the process of data block allocation for supporting the prefetch mechanism.

Within each leaf node, we try to store as many data points in the predicted data block as possible, to increase the success rate of prefetch. This corresponds to another optimization problem within the leaf node.

5.3.3 *The Prefetch Prediction Model.* To learn the prefetch prediction model, we also establish a cost model for it and optimize accordingly. Let $L = \{M_1, \dots, M_n\}$ be the collection of leaf nodes directly under the root node, then the cost of index accesses on these nodes can be approximated as:

$$\sum_{i=1}^n \left[\frac{|Q_{M_i}|}{|Q|} \mathbb{E}_{q \in Q_{M_i}} [TCost(M_i, q)] + \lambda SCost(M_i) \right] \quad (9)$$

where Q_{M_i} is the collection of queries accessing M_i .

Considering the effect of prefetching, the time cost of data blocks becomes slightly different. a leaf node that supports prefetch (i.e., allocated to its predicted location), the time cost of accessing data blocks is now equal to the latency of cache memory, and the value of $TCost(M_i, q)$ also changes accordingly. This downside is that now $SCost(M_i)$ can be slightly larger than needed.

We use a dynamic programming algorithm to optimize Equation 9. The DP state $cost[i, r]$ is the total cost of first r leaf nodes when we use i segments to model them. This is a standard 2D dynamic programming and we omit the algorithm details here.

workloads	indexes	uniform dataset			lognormal dataset			YCSB dataset		OSMC dataset			Face dataset		
		space /MB	time /ns		space /MB	time /ns		space /MB	time /ns	space /MB	time /ns		space /MB	time /ns	
			uniform	zipfian		uniform	zipfian				uniform	zipfian		uniform	zipfian
read-only	CARMI	1394.3	114.3	85.1	1475.7	129.2	92.1	11.4*	93.2	1771.5	287.5	160.1	1812.6	248.5	166.4
	ALEX	1474.3	112.5	83.3	1476.7	115.5	89.3	1474.3	97.6	1522.0	421.9	221.4	1522.0	404.0	228.1
	B-Tree	2276.0	482.6	267.8	2276.0	480.6	268.1	2276.0	269.7	2276.0	479.9	262.5	2276.0	480.6	261.5
write-heavy	CARMI	1509.9	168.4	154.5	2127.4	190.3	168.6	11.4*	161.2	1772.5	357.9	246.0	1882.7	316.9	246.2
	ALEX	1474.3	164.1	147.0	1476.7	294.0	262.9	1474.3	317.3	1522.0	1109.1	893.3	1522.0	1801.7	1777.6
	B-Tree	2276.0	500.3	419.9	2276.0	522.4	421.9	2276.0	401.2	2276.0	503.5	421.3	2276.0	498.7	432.9
read-heavy	CARMI	1509.4	135.8	102.1	2077.5	155.0	104.2	11.4*	104.4	1771.9	330.2	172.5	1812.9	278.3	174.2
	ALEX	1474.3	116.2	89.2	1476.7	121.7	95.4	1474.3	234.7	1522.0	651.7	420.4	1522.0	993.8	829.0
	B-Tree	2276.0	488.9	286.8	2276.0	483.4	292.5	2276.0	280.4	2276.0	483.1	284.5	2276.0	477.6	280.1
write-partial	CARMI	1509.9	156.9	117.3	2082.5	162.8	121.5	11.4*	124.5	1772.2	341.6	179.5	1853.8	286.2	184.0
	ALEX	1474.3	130.4	109.8	1476.7	190.4	180.1	1474.3	285.0	1522.0	854.7	588.5	1522.0	1240.6	1092.4
	B-Tree	2276.0	490.1	318.8	2276.0	488.2	321.4	2276.0	311.2	2276.0	487.3	314.4	2276.0	483.2	314.5
range scan	CARMI	1509.4	402.4	256.4	2077.5	434.3	271.3	11.4*	266.4	1771.9	585.6	305.3	1812.9	600.9	323.9
	ALEX	1474.3	375.0	233.6	1476.7	383.6	240.3	1474.3	359.3	1522.0	935.3	598.2	1522.0	1246.4	990.5
	B-Tree	2276.0	704.5	416.5	2276.0	728.5	414.7	2276.0	393.1	2276.0	696.4	417.1	2276.0	698.7	415.3

* Does not include the space of external array.

Figure 10: CARMI vs. Baselines: Time and Space Usage Comparison.

6 EXPERIMENTS

In this section, we conduct experiments on various datasets and workloads to evaluate the performance of CARMI and delve into CARMI from different aspects through several auxiliary experiments.

6.1 Experimental Setup

We conducted all the single-threaded experiments on an Ubuntu Linux machine equipped with an AMD Ryzen 3700X 8-Core Processor and 32GB RAM.

6.1.1 *Datasets.* Seven datasets are used in our main experiments. Their details are listed as follows:

- **synthetic dataset:** 4 synthetic datasets are generated from 4 different distributions: (a) **lognormal:** $\log(key) \sim \mathcal{N}(0, 1)$; (b) **uniform:** $key \sim \mathcal{U}(0, 1)$; (c) **normal:** $key \sim \mathcal{N}(0, 1)$; (d) **exponential:** $key \sim \text{Exp}(0.25)$. All these datasets are stored as key-value pairs of $\langle double, double \rangle$. The size of each dataset is 1GB, and the key values of data points are multiplied by 10^8 .
- **YCSB dataset:** This dataset consists of 67,108,864 data records generated by YCSB benchmark [14]. We build an index on the YCSB_KEY attribute, which obeys a uniform distribution.
- **OSMC dataset:** This dataset is generated from a public dataset of Open Street Maps [2], which includes the latitude and longitude of points around the world. The number of data points in this dataset is 67,108,864 (the size of each dataset is 1GB). This dataset is stored as key-value pairs of $\langle uint64, uint64 \rangle$.
- **Facebook dataset:** This dataset is generated from the IDs of Facebook users [24, 51], consisting of 67,108,864 data points. This dataset is stored as key-value pairs of $\langle uint64, uint64 \rangle$.

We have also ported CARMI into the SOSD [24] platform to test its performance and the details are shown in Section 6.3.

6.1.2 *Evaluation Workloads.* We use 5 different query workloads in our experiments. The first three workloads are similar to the workloads in the YCSB benchmark [14]: (a) a write-heavy workload with a mix of 50% reads and 50% inserts; (b) a read-heavy workload with a mix of 95% reads and 5% inserts; (c) a read-only workload. In addition, we include a write-partial workload in which insert

operations are concentrated in a small key value range. This workload consists of 85% reads and 15% inserts, and the inserted data points are concentrated between 60% and 90% of the sorted dataset. The write-partial workload is intended to mimic some real-world scenarios in which the keys of new data points are contained in a small value range during each session (e.g., when using the current date/time as key value). Finally, we include a range scan workload with a mix of 95% range scan and 5% inserts as in [16].

For each workload, we execute 100,000 operations and measure the average time used by each operation. For all workloads, lookup keys are selected at random from the existing keys in the index. We consider two access patterns for generating queries: a Zipfian distribution (the normalized frequency of the x -th element is: $f(x) = \frac{1}{x^\alpha} / \sum_{i=1}^N \frac{1}{i^\alpha}$, $\alpha = 0.99$ as in [16]) and a uniform distribution. In workloads involving insert operations, read and insert operations are performed alternately in proportion. For example, in read-heavy workloads, we execute 19 lookups followed by 1 insert operation. For range scan workloads, the length of each range scan is uniformly sampled from [1, 100].

For the YCSB dataset, the queries are handled differently to simulate real-world use cases: read queries are generated from a Zipfian distribution as usual, but insert keys are monotonically increasing to be consistent with the YCSB benchmark.

6.1.3 *Implementation and Baseline.* We compare against the following baselines: STX B+ Tree [3] and ALEX [16]. The node size of B+ Tree is 512 bytes, which is optimal for in-memory queries [55]. All other parameters use the default values in the source code. SOSD benchmark [24] also includes some other indexes as baselines in Section 6.3. CARMI is open-sourced and can be found on Github [1]. In our experiments, we only tune one parameter λ , which is sensitive to data distribution and dataset size, and all other parameters do not need to be tuned and use the default values unless otherwise stated. More details can be found in the appendix.

6.1.4 *Training Queries for Index Construction in CARMI.* In our experiments, the training query workload for index construction is specified as a uniform read access over all data points, and a uniformly sampled subset of data points³ to serve as key values for

³The insert queries in the training queries of the write-partial workload are sampled between 60% and 90% of the overall dataset.

insert queries (with the exception of YCSB dataset). The ratio of read/insert queries is the same as in the target query workload.

6.2 General Efficiency Comparison

In this section, we evaluate the performance of CARMi and compare it with the baselines. We consider 5 query workloads and 7 different datasets, as explained in Section 6.1. We consider two access patterns for datasets other than YCSB: uniform and Zipfian, as illustrated in Section 6.1.2. These result in a total of 65 possible configurations. Figure 10 shows the results for 45 of them due to space limitation, and the results for normal and exponential datasets are omitted since they are similar to those of the uniform dataset.

In general, the time efficiency of both learned indexes is significantly better than B+ Tree. Comparing CARMi with ALEX, which is also a learned index, we see that these two learned indexes perform roughly the same over synthetic datasets. However, CARMi significantly outperforms on these real-world datasets, achieving an average speedup of 1.2×/2.2× on read-only/read-write workloads. This demonstrates the effectiveness of data partitioning and cache-aware design over real-world datasets, in which data location is much harder to predict.

6.2.1 Read-only Workload. For read-only workloads, the lookup speed of CARMi is about 1.6-4.2× faster than B+ Tree, and 1.2× faster on average than ALEX. Meanwhile, CARMi uses only 0.7× of memory space compared to B+ Tree (excluding YCSB⁴ dataset).

It is of interest to compare CARMi with B+ Tree, since their difference is only on the upper level. The significant speed gain of CARMi is mainly due to the following reasons: (a) CARMi uses fast model prediction instead of binary search. (b) the larger fanout of the root nodes in CARMi reduces the depth of the index. Then, most of the data points are managed by a leaf node that is directly under the root node, making the index structure flatter. To verify that our construction algorithm can build a flatter index, we also calculated the average tree depth with respect to keys, where a single root node has a depth of 1. The average tree depth of CARMi is 2.1, while that of ALEX and B+ Tree are 2.5 and 7.3, respectively.

Comparing the two learned indexes, the main difference is in the performance over OSMC/Face, in which CARMi achieves an average speedup of 1.5×. The two datasets are real-world datasets with highly non-linear local distribution (the CDFs can be found in Figure 11), which invalidates ALEX’s strategy of storing data points according to the predicted location, and causes the index to grow deeper. Meanwhile, our hybrid construction algorithm can automatically select suitable nodes to obtain better performance. Section 6.3 shows similar results on other real-world datasets as well, making it clear that this is not a coincidence.

In summary, CARMi outperforms B+ Tree and can achieve similar or better performance than ALEX under read-only workloads, and the gain is more evident on real-world datasets.

6.2.2 Write-heavy Workload. CARMi achieves an average speedup ratio of 2.2× compared to B+ Tree and 3.0× compared to ALEX⁵ on write-heavy workloads.

It is generally difficult for learned indexes to divide non-linear datasets evenly, leading to a large gap between the numbers of data points in each node. This results in additional expansion costs in ALEX during the insert operations. However, CARMi handles well even under such scenarios, using only 0.42× time of ALEX on lognormal/real-world datasets. As for space cost, CARMi uses 1.2× space compared to ALEX, and 0.8× compared to B+ Tree on average.

In summary, CARMi has a better time efficiency and uses a similar amount of space compared to ALEX, and the gap is more significant on non-linear and real-world datasets.

6.2.3 Other Read-Write Workloads. CARMi has a shorter access time (2.04×/2.03× average speedup compared to B+ Tree and ALEX respectively) and use less space (0.79× on average compared to B+ Tree) for all other read-write workloads including range scan workload. This shows that CARMi can better handle various workloads, especially non-linear datasets.

6.3 SOSD Results

In order to further test the performance of CARMi on real-world datasets, we have integrated CARMi into the SOSD benchmark [24, 36], a platform for testing learned index structures. We use all real-world datasets in SOSD, each of which consists of 200 million unsigned 32-bit/64-bit integers: **amzn** is book sale popularity data [4], **face** is the IDs of Facebook users [51], **wiki** is Wikipedia article edit timestamps [5], and **osmc** is generated from a public dataset of Open Street Maps [2]. SOSD performs 10 million lookups on each dataset, where the lookup keys are uniformly chosen from the set of keys, and computes the average latency per lookup.

There are 10 baselines in SOSD and are categorized into four types: (a) **three learned indexes**: RMI, RS and ALEX; (b) **three traditional indexes**: B+ Tree, FAST and ART; (c) **three on-the-fly algorithms** that directly operate on a sorted array: BS, IS and TIP; (d) **one auxiliary index** that uses small auxiliary structures: RBS. Among them, FAST and ART do not support all the datasets as explained in SOSD and more details can be found in [24]. Table 3 shows the average lookup time of indexes on **all real-world datasets** in the SOSD benchmark, where the results with the shortest latency and those slightly slower (within 20ns) are bolded.

We also examine the distribution of datasets. As shown in Figure 11, a major difference between synthetic and real-world datasets is that synthetic datasets all have locally linear CDF, which is rare in real-world datasets. The highly non-linear local CDFs of real-world datasets make it difficult for prior solutions to predict the location of individual data records accurately, leading to large-range searches in the last mile. In contrast, because CARMi is designed based on the data partitioning view with a more cache-friendly leaf node layout, it is less penalized by these highly non-linear parts and thus performs better in real-world datasets: CARMi can achieve an average speedup of 1.21× even compared to a well-tuned RMI.

⁴For the YCSB dataset, since CARMi uses the external leaf nodes, which only store a pointer of the location of data points, the space cost of 11.4 MB only counts the space of the tree structure itself and does not include the space used by external data.

⁵The insert of the YCSB protocol is to continuously insert new data points at the end of the dataset, and ALEX does not strictly follow this mode for insert in their paper. Thus, our reported number is different compared to the values in their paper.

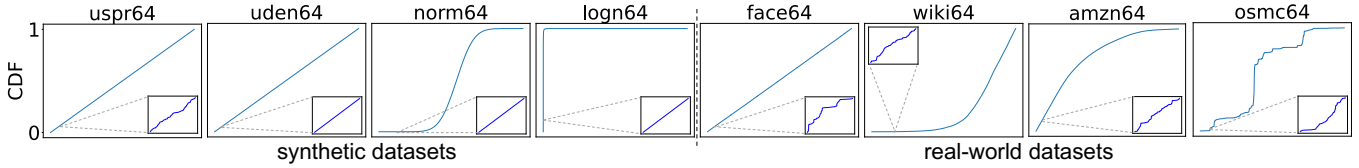


Figure 11: The CDFs of Datasets in SOSD [24].

Table 3: The Average Lookup Time (ns) on SOSD Platform.

(ns)	uint32		uint64			
	amzn	face	amzn	face	wiki	osmc
CARMI	192.84	187.43	201.80	334.41	217.50	368.65
RMI	265.43	274.53	266.54	334.54	222.43	402.32
RS	280.03	362.54	296.61	436.63	218.43	412.39
ALEX	210.99	434.69	251.32	496.48	289.81	499.04
RBS	325.43	312.39	385.96	334.73	335.75	529.06
FAST	246.03	228.79	N/A	N/A	N/A	N/A
ART	N/A	182.36	N/A	391.76	N/A	N/A
B+Tree	529.43	524.54	601.23	592.43	608.42	599.43
BS	1014.5	983.49	1015.1	961.93	1002.3	987.24
TIP	731.97	880.12	750.89	1124.6	942.84	4773.8
IS	3852.7	1007.7	4103.9	1494.8	6836.4	66474

Interestingly, most learned indexes do not perform better than traditional indexes on particular real-world datasets, as shown in Table 3. Specifically, FAST takes only 237.41 ns on average on amzn32 and face32, while RMI, RS, and ALEX take $1.14\times/1.35\times/1.36\times$ average lookup time, respectively. ART takes an average of 287.06 ns on face32 and face64, while RMI, RS, and ALEX take $1.06\times/1.39\times/1.62\times$, respectively. Despite that, the lookup latency of CARMI is robust enough to be the shortest or very close to the shortest among all indexes for all datasets.

We also report the average space usage of each index in Table 4. The space required by CARMI is comparable to that of traditional indexes with good performance, such as FAST and ART. Note that the space cost of CARMI can be adjusted by users.

Table 4: Average Space Usage (MB) on SOSD.

	CARMI	RMI	RS	ALEX	RBS	
uint32	3918.30	2471.65	2299.63	3336.74	2289.82	
uint64	5481.44	3143.31	3064.33	4430.83	3052.76	
	FAST	ART	B+Tree	BS	TIP	IS
uint32	5120.00	4596.52	2657.31	2288.82	2288.82	2288.82
uint64	N/A	5280.92	3540.52	3051.76	3051.76	3051.76

6.4 Tradeoff between Time and Space

One additional advantage of our cost-based index construction algorithm is that one can now flexibly choose the balance point between time and space cost. As shown in Figure 12, by tuning the value of parameter λ in Problem 2, one can reduce the memory usage of indexes at the cost of increased read access latency. The curves of real-world datasets exhibit the characteristics of convex functions, but the optimal solution for each dataset depends on the actual data distributions. Therefore, we need to carefully tune λ

according to practical scenarios to find the optimal solution, so as to obtain a more desired tradeoff between time and space.

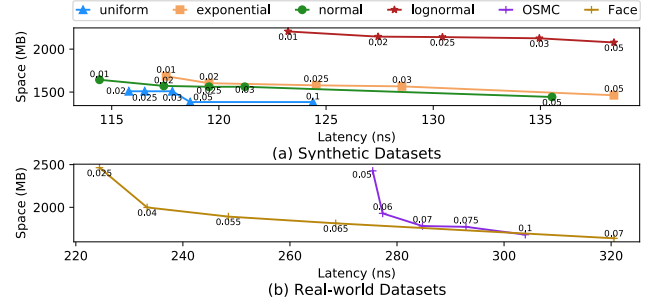


Figure 12: The Tradeoff Between Time and Space Cost

6.5 Cost of Construction

The construction of the index structure should only be performed periodically when the database system has enough computation resources to spare (e.g., during night time when the frequency of the incoming queries is low). As such, the time efficiency of the construction algorithm is not a major concern. Nevertheless, we still want to have a basic understanding of its time cost.

Recall that we have two algorithms (the greedy algorithm and the DP algorithm) to construct a node. In order to achieve a balance between the construction time and the average lookup latency, we define a parameter $kDPT_{threshold}$ in CARMI, and use the greedy algorithm when the size of the sub-dataset is greater than the parameter. As shown in Figure 13, the construction of CARMI with different values of $kDPT_{threshold}$ can be finished within 0.3-3.2 minutes, while B+ Tree and ALEX take 10s and 20s on average, respectively. Although CARMI takes longer to build indexes than baselines, it is generally acceptable for most practical scenarios. Moreover, the value of this parameter has a slight impact on the average lookup latency, with the difference between a value of 96 and 1024 being around 10 ns.

To conclude, in scenarios where construction time is more important, $kDPT_{threshold}$ can be tuned to reduce the construction time. While in most practical scenarios, the default value can be used directly.

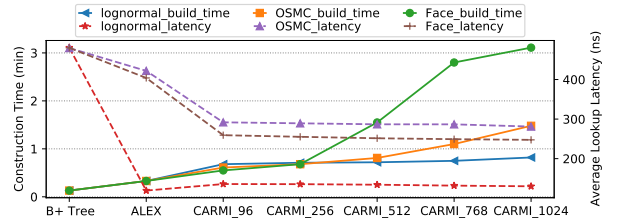


Figure 13: Construction/lookup Time of Indexes.

Table 5: Statistics on Different Root Fanouts.

Root Fanout	Uniform Dataset			Normal Dataset			Lognormal Dataset			OSMC Dataset		
	Time /ns	# of Accesses	Percentage	Time /ns	# of Accesses	Percentage	Time /ns	# of Accesses	Percentage	Time /ns	# of Accesses	Percentage
65536	301.64	6.82	5.14%	355.39	7.67	4.76%	372.72	8.73	3.32%	593.10	11.95	0.22%
131072	280.58	5.72	7.28%	333.46	6.66	6.74%	337.73	7.69	4.68%	539.83	11.15	0.38%
262144	254.16	4.62	10.36%	300.26	5.65	9.58%	308.69	6.64	6.62%	487.83	10.33	0.67%
524288	212.34	3.52	14.66%	276.09	4.65	13.55%	283.86	5.58	9.35%	449.08	9.52	1.14%
1048576	168.43	2.47	20.66%	232.51	3.68	19.05%	261.56	4.54	13.05%	410.11	8.69	1.89%
2097152	152.71	1.53	28.64%	212.36	2.80	26.25%	230.68	3.53	17.99%	374.43	7.85	3.05%

6.6 The Effect of Fanout

In order to show the effect of root fanout on average access time, we use CARMi to simulate a two-layer static RMI with adjustable root fanout. The root node, which is the linear regression model, directly manages the leaf nodes. Each leaf node is an external array leaf node. Table 5 shows the average access time and the average number of memory accesses required per query under different root fanouts. We also count the percentage of data points that are stored in the same location as the location calculated by the linear model across all data points.

As demonstrated in Table 5, the average access time tends to be smaller as the fanout increases. The gains are particularly evident on non-linear datasets like the OSMC dataset. The benefits brought by a large fanout are mainly due to the following reasons: (a) It reduces the number of data points in each leaf node and thereby avoids the occurrence of a wide range of binary searches, resulting in the reduced number of memory accesses. (b) It can simplify the situation of lower-level nodes, so that more data points can have their actual storage positions to be consistent with the calculation results of the linear model.

In general, a larger fanout of the root node can reduce the average access time to some extent. Its contribution to the local efficiency of the root node is quantified in our entropy metric, which further validates our view of data partitioning.

6.7 Performance Breakdown

In this section, we examine the performance improvements brought by each design.

6.7.1 Detailed Performance Study. First, we investigate the contribution of each idea to the overall performance. We implement 4 variants of CARMi to simulate indexes with different ideas and perform read-only workloads on 5 datasets, including 3 synthetic datasets and 2 real-world datasets. A brief introduction of these variants are as follows:

- **RMI:** a two-layer RMI with an LR root node and 131072 external leaf nodes.
- **Greedy:** a dynamic index constructed by the greedy algorithm.
- **Greedy cache-aware:** a dynamic index equipped with the cache-aware design and greedy algorithm.
- **CARMi:** a complete CARMi equipped with all proposed ideas.

As shown in Figure 14, most of the advantages of the CARMi framework come from the data partitioning view, which enables the greedy index to achieve an average speedup of 1.84× compared to RMI. Specifically, only the greedy algorithm is used to build the

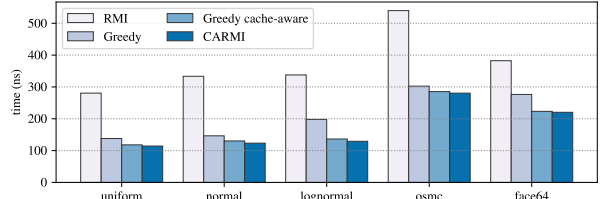


Figure 14: Latency of Four CARMIs.

index, so each node setting is determined by the entropy-based notion of local efficiency. This means that nodes can have larger fanouts for smaller sub-datasets, reducing large-range searches in RMI. In addition, four inner nodes can be mixed to handle different situations well to obtain better data partitioning effectiveness.

Next, in the greedy cache-aware index, we replace leaf nodes with CF array leaf nodes and cooperate with the prefetching mechanism to examine the effect of our cache-aware design. Due to the influence of data distributions and different sub-datasets partitioned by the greedy algorithm, the cache-aware design shows different effects. Among them, the speedup for lognormal and face64 datasets is more significant. In summary, this index still obtains an average speedup of 1.21× compared to the greedy index, which is the contribution of cache-aware design.

If resources are sufficient, users can use the hybrid construction algorithm consisting of the greedy algorithm and DP algorithm to build better indexes. According to the average access time when parameter $kDPThreshold$ is 1024, as shown in Figure 14, the complete CARMi can reduce the average access time by about 10ns.

6.7.2 Model Characteristics. Next, we investigate the effect of using four inner nodes flexibly in the index. First, we conduct experiments on the four inner nodes to show their respective characteristics. In these experiments, the root nodes are all piecewise linear nodes, but we only allow one kind of node to be used as inner nodes. In addition, the results of CARMi are also shown in Table 6, where the hybrid algorithm flexibly uses these four inner nodes.

Table 6: Latency on Different Model Types.

Latency /ns	LR	P. LR	Hist	BS	CARMi
Uniform	136.8	143.5	141.3	145.8	136.6
Normal	153.6	152.5	158.7	154.9	139.4
Logn	157.5	155.0	155.8	153.8	139.9
OSMC	415.8	405.3	413.32	374.9	293.4

As shown in Table 6, CARMi outperforms the indexes formed by using these nodes individually, indicating that the mixed-use of

these four different types of models can effectively speed up the query response. More specifically, on the one hand, LR nodes can handle evenly distributed parts well, thus beating other models on the uniform dataset. On the other hand, for the non-linear part, the PLR and Hist nodes sacrifice some model calculation time in exchange for better data partitioning results. As for the extreme case, BS node can handle it well. Although the model computation takes more time, as shown in Table 2, it can partition the OSMC dataset more evenly, resulting in a shorter average access time.

In summary, it makes sense to combine different nodes together and can be easily achieved based on our fixed-size node design. CARMi benefits from our hybrid construction algorithm and cost model to select optimal node settings in different situations to get the shortest average access time.

6.7.3 Prefetching Mechanism. In order to evaluate the impact of the prefetching mechanism, we conduct experiments with and without prefetching instructions on these four datasets and show the time/space costs and the proportion of data blocks that are successfully prefetched in Table 7. On these synthetic datasets, the average success rate of the prefetching mechanism is 93.1%, and the average access time is reduced by 63.1 ns. For real-world datasets, most data points require at least two inner nodes to handle the data distribution, so there is little gain in prefetching them at the root node. As we discussed in Section 5.3, the prefetching mechanism requires more space to better exert its effects.

Table 7: Results With/Without Prefetch Mechanism.

	with prefetch			without prefetch	
	time/ns	space/MB	proportion	time/ns	space/MB
Uniform	114.0	1509.3	98.3%	185.8	1230.6
Normal	124.6	1561.6	89.1%	184.4	1334.2
Logn	126.2	2137.8	91.9%	183.7	1912.4
OSMC	284.5	1557.86	2.5%	289.3	1533.4

6.8 Robustness of CARMi

In this section, we simulate three groups of workload and data distribution shifts to examine the robustness of CARMi.

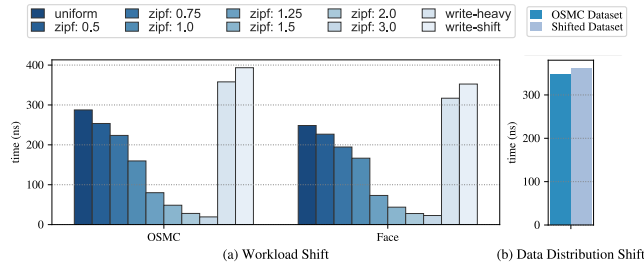


Figure 15: Robustness of Indexes in Different Situations.

6.8.1 Workload Shift. First, we examine whether CARMi can cope with read-only workload shifts. We construct indexes from evenly distributed historical queries on OSMC/Face datasets, and query them with 8 different access patterns: seven Zipfian distributions ($f(x) = \frac{1}{x^\alpha} / \sum_{i=1}^N \frac{1}{i^\alpha}$, $\alpha \in \{0.5, 0.75, \dots, 1.5, 2, 3\}$) and a uniform

distribution as a baseline. The average access time of Zipfian indexes decreases with the increase of α and is smaller than that of the baseline, as shown in Figure 15(a). The results show that CARMi is robust and can handle read-only workload shifts well.

Then, we construct indexes with historical queries under read-heavy and write-heavy workloads, respectively, and test them with write-heavy workloads. Although the indexes built on read-heavy workloads require $1.1\times$ the average time compared to indexes built on write-heavy workloads, as shown in Figure 15(a), CARMi still executes queries quickly and is robust to workload shifts.

6.8.2 Data Distribution Shift. Next, we demonstrate the robustness of CARMi to data distribution shifts. We first use the uniform dataset with 67,108,864 key values to build indexes, and then perform a write-heavy workload using 67,108,864 data points from OSMC dataset. Since inserted data points come from a different dataset, we can simulate the situation where the data distribution gradually changes from a uniform distribution to a non-linear distribution. Figure 15(b) shows that although CARMi requires slightly more average time than the index built on OSMC dataset, CARMi can still maintain good performance in this situation. But we still recommend that if data distributions change significantly, reconstruction should be done in time for better performance when sufficient resources are available.

6.9 Tree Structure

To understand the behavior of the index construction algorithm, we have gathered statistics on the optimal indexes constructed by the algorithm, and some of them are shown in Table 8. We follow the convention that the depth of a trivial tree (with only root node) is 1, and count depth on the leaf node level. The average is calculated with respect to keys.

Table 8: Statistics of Indexes Constructed by CARMi.

node	read-only		lognormal	
	uniform	normal	write-heavy	write-partial
root node	LR	P. LR	P. LR	P. LR
# of children	1175653	1175653	1528348	1528348
# of LR	2	835	4690	4697
# of P. LR	0	4	8	8
# of Hist	0	2	2	0
# of BS	0	0	0	1
Array	1175685	1320524	1784066	1767682
Max Depth	3	3	4	4
Avg Depth	2	2.03	2.07	2.07

The first two columns are statistics under a read-only workload. As we can see, the algorithm constructs an average two-layer structure for uniform dataset under read-only workloads: the first layer is the LR root node and the second layer are the CF array leaf nodes. When performing a read query, we only need to access a single leaf node and a single data block. Due to the distributional variation caused by the sampling process, a small number of data points need an additional inner node.

For other datasets, we can no longer construct a simple two-layer index to handle the dataset as the data points are very concentrated in a specific range, which cannot be handled by a single leaf node. As we can see, the root node setting changes depending on the data distribution and CARMi chooses to use P. LR for all the other three scenarios. We also see that the algorithm generates new inner nodes to partition the data points further, and builds deeper subtrees in more concentrated parts of the data points. Aside from the deep part, the algorithm maintains a shallow free structure in the other parts to guarantee that the average depth is small, achieving an average depth of 2.03-2.07.

As we can see in Table 8, depending on the data distribution, the algorithm will adaptively use the four types of inner nodes. For example, in lognormal dataset under write-partial workload, CARMi constructed 4697 LR nodes in the evenly distributed part, and 8 P. LR nodes in the unevenly distributed part. In general, CARMi can effectively handle different data distributions and diverse workloads, and construct a reasonable index structure accordingly. These results also justify the decision of including multiple tree node types in CARMi, which enhances the flexibility of index structures.

7 DISCUSSION AND FUTURE WORK

7.1 CARMi in Disk/NVM

In our current implementation of CARMi, both inner nodes and leaf nodes are stored in memory. We can easily extend CARMi to involve disk operations. If we store data points on disk, we need to design a new type of leaf node that accesses a disk page instead of an in-memory data block. The corresponding time and space costs of this new type of node should also reflect the latency of disk operations. The current hybrid construction algorithm can be directly used without any change.

Moreover, with the rapid development of non-volatile memory (NVM) [30], the capacity of memory can be vastly expanded while still retaining decently high access speed. The difference in access latency of heterogeneous storage devices can be characterized by modifying the cost model of CARMi, and the construction algorithm will be able to accommodate the new hardware properly.

7.2 Other Data Types

In our implementation of CARMi, we only support numerical key types. It is possible to extend CARMi to handle other types as well. Generally speaking, the existing RMI framework cannot readily handle strings since the distribution of strings is hard to fit well by their current models. Our perspective based on data partition can potentially address this difficulty. It is necessary to design new nodes for strings and make certain changes to the storage method. For the hybrid construction algorithm and the overall cost model, we need to make minor changes to them, but ideas and processes of the original algorithm can still be applied.

7.3 Concurrent Operations

There have been many methods and implementations on concurrency control of indexes, including B+ Tree [9, 20, 40, 48]. The overall structure of CARMi is similar to B+ Tree, and it is also in the form of a tree composed of multiple different nodes. Therefore, the traditional concurrency control method can also be used on

CARMi. We can use read/write locks to support concurrency. For lookup operations, we only need to obtain the read locks of the leaf node and its upper layer node when traversing the index. For insert operations, we obtain the write locks on the nodes in the access path. If the leaf node can handle the insert operation without the need for split operation, the lock of the upper nodes can be released.

8 RELATED WORK

In this section, we introduce some related works in the field of database index.

Traditional Indexes: Many researchers have optimized index structures in the past decades and have proposed many indexes to achieve good performance, such as B-tree, B+ tree [7, 8], T tree [31], balanced B-tree [6] and red-black tree [12], etc. Since most indexes are stored in the main memory, CSS-tree [46] restricts node size to the cache line size and eliminates child nodes' pointers to utilize the cache and CSB+ tree [47] is then proposed to support updates. ART [32] is an adaptive cardinality tree designed to reduce the number of cache misses. For further acceleration, pB+-tree [13] and FAST [22] use prefetching instructions and SIMD instructions, respectively. Masstree [35] effectively handles possible binary keys of any length, including keys with long shared prefixes.

Learned Indexes: Kraska et al. [27] propose a recursive model index (RMI), which uses ML models instead of index structures represented by B-tree. However, RMI does not support inserts. Fiting-tree [19] uses linear models to replace the leaf nodes of B-tree to compress the index. PGM-index [18], a compressed learned index with provable worst-case bounds, extends Fiting-tree and provides an optimal method to find the piecewise linear models. These two indexes support inserts by additional buffers, and the performance needs to be improved. To support writes, ALEX [16] uses model-based inserts and gapped array leaf nodes to make room for future inserts. However, ALEX requires large-range searches to accurately locate data points, resulting in performance degradation on real-world datasets. In this paper, we adopt a data partitioning view and use a cost-based hybrid construction algorithm to select suitable node settings to build an updatable index. CARMi makes full use of various types of nodes to handle different situations, thus maintaining good performance on real-world datasets.

CDFShop [38] uses Pareto analysis to find Pareto optimal configuration for the static two-layer RMI. They use a parameter search strategy, which is not suitable for dynamic structures due to the exponentially large number of configurations in the search space. On the other hand, CARMi can automatically tune tree structures and model types at runtime through a new dynamic architecture and the cost-based algorithm.

Besides, RadixSpline [25] focuses more on building indexes in single pass and PLEX [49] is built on RS and retains only one hyperparameter for more convenient use. LIPP[53] uses entry types and a conflict degree metric to decide tree node layout. Mitzenmacher et al. [39] build a learning bloom filter that uses neural network models to predict whether keywords belong to a certain set. In addition, there are several other works that apply the idea of the learned index to multi-dimensional indexes [17, 41] and spatial query processing [33, 43, 45, 52] to improve performance.

Other Applications of ML in Database: In other parts of the database, many novel ideas that utilize ML techniques have also been proposed. Park et al. [44] applied ML techniques to approximate query processing. They found that the answer to each query revealed some degree of knowledge about the answer to another query. Because their answers come from the same underlying distribution that produced the entire dataset. Therefore, it is possible to use ML techniques to improve this knowledge and answer questions in a more organized manner instead of reading a lot of raw data. In addition, several research teams [23, 29, 37, 42, 50, 54] proposed the use of reinforcement learning, CNN, DNN and other AI related models to predict cardinality and optimize queries.

Cumin et al. [15] proposed a rewriting technique of SQL query based on ML. This technology can help data scientists formulate SQL queries and browse big data quickly and intuitively. At the same time, the user input can be minimized without manual tuple description or marking.

Kraska et al. proposed a blueprint of a database that uses ML techniques in each part [26, 28] to improve performance and discussed several ideas for designing new benchmarks [11] for learned systems. ADCP [34], an active data collection platform, and HAL [34], a novel active learning technique to gather data in the database, are applied to handle the problem of performance degradation of ML models in use.

9 CONCLUSION

This paper conducts in-depth research on the basic framework of learned indexes (RMI), and argues that the inflexibility of data partitioning is an important reason for the performance degradation of RMIs in practical scenarios. To address this issue, we propose to view RMI construction from a data partitioning view and propose a general cache-aware RMI framework, called CARMi. Specifically, we use the entropy metric to quantify the data partitioning effectiveness and propose a new cost model to characterize the performance of individual tree nodes, which helps to design more robust indexes. Furthermore, CARMi is equipped with a new memory layout that is more cache-friendly and uses a hybrid algorithm to automatically construct index structures for different datasets and workloads without manual tuning. Experimental results show that CARMi has an outstanding performance under a variety of datasets and workloads, achieving an average of $2.2\times/1.9\times$ speedup compared to B+ Tree/ALEX, respectively, while using only $0.77\times$ the memory space on average. This paper demonstrates that data partitioning is important for learned indexes during construction and that the new cost model can well characterize the performance of a single node, which is beneficial to improving the performance and flexibility of indexes. Finally, the CARMi framework is highly extensible and robust, and can be applied to a wider range of scenarios if we design different types of nodes for it.

REFERENCES

- [1] [n.d.]. https://github.com/JiaoYiZhang/learned_index.
- [2] [n.d.]. <https://registry.opendata.aws/osm/>.
- [3] [n.d.]. <https://panthema.net/2007/stx-btree/>.
- [4] [n.d.]. <https://www.kaggle.com/ucfool/amazon-sales-rank-data-for-print-and-kindle-books>.
- [5] [n.d.]. <http://dumps.wikimedia.org>.
- [6] Rudolf Bayer. 1972. Symmetric binary B-trees: Data structure and maintenance algorithms. *Acta informatica* 1, 4 (1972), 290–306.
- [7] R Bayer and E McCreight. 1970. ORGANIZATION AND MAINTENANCE OF LARGE. (1970).
- [8] Rudolf Bayer and Edward McCreight. 2002. Organization and maintenance of large ordered indexes. In *Software pioneers*. Springer, 245–262.
- [9] Rudolf Bayer and Mario Schkolnick. 1977. Concurrency of operations on B-trees. *Acta informatica* 9, 1 (1977), 1–21.
- [10] Brian Beavis and Ian Dobbs. 1990. *Optimisation and stability theory for economic analysis*. Cambridge university press.
- [11] Laurent Bindschaedler, Andreas Kipf, Tim Kraska, Ryan Marcus, and Umar Farooq Minhas. 2021. Towards a Benchmark for Learned Systems. In *2021 IEEE 37th International Conference on Data Engineering Workshops (ICDEW)*. IEEE, 127–133.
- [12] Joan Boyar and Kim S Larsen. 1994. Efficient rebalancing of chromatic search trees. *J. Comput. System Sci.* 49, 3 (1994), 667–682.
- [13] Shimin Chen, Phillip B Gibbons, and Todd C Mowry. 2001. Improving index performance through prefetching. *ACM SIGMOD Record* 30, 2 (2001), 235–246.
- [14] Brian F Cooper, Adam Silberstein, Erwin Tam, Raghu Ramakrishnan, and Russell Sears. 2010. Benchmarking cloud serving systems with YCSB. In *Proceedings of the 1st ACM symposium on Cloud computing*. 143–154.
- [15] Julien Cumin, Jean-Marc Petit, Vasilie-Marian Scuturici, and Sabina Surdu. 2017. Data exploration with sql using machine learning techniques.
- [16] Jialin Ding, Umar Farooq Minhas, Jia Yu, Chi Wang, Jaeyoung Do, Yinan Li, Hantian Zhang, Badrith Chandramouli, Johannes Gehrke, Donald Kossmann, et al. 2020. ALEX: an updatable adaptive learned index. In *Proceedings of the 2020 ACM SIGMOD International Conference on Management of Data*. 969–984.
- [17] Jialin Ding, Vikram Nathan, Mohammad Alizadeh, and Tim Kraska. 2020. Tsunami: A learned multi-dimensional index for correlated data and skewed workloads. *arXiv preprint arXiv:2006.13282* (2020).
- [18] Paolo Ferragina and Giorgio Vinciguerra. 2020. The PGM-index: a fully-dynamic compressed learned index with provable worst-case bounds. *Proceedings of the VLDB Endowment* 13, 8 (2020), 1162–1175.
- [19] Alex Galakatos, Michael Markovitch, Carsten Binnig, Rodrigo Fonseca, and Tim Kraska. 2019. Fiting-tree: A data-aware index structure. In *Proceedings of the 2019 International Conference on Management of Data*. 1189–1206.
- [20] Goetz Graefe and Harumi Kuno. 2011. Modern B-tree techniques. In *2011 IEEE 27th International Conference on Data Engineering*. IEEE, 1370–1373.
- [21] Robert M Gray. 2011. *Entropy and information theory*. Springer Science & Business Media.
- [22] Changkyu Kim, Jatin Chhugani, Nadathur Satish, Eric Sedlar, Anthony D Nguyen, Tim Kaldewey, Victor W Lee, Scott A Brandt, and Pradeep Dubey. 2010. FAST: fast architecture sensitive tree search on modern CPUs and GPUs. In *Proceedings of the 2010 ACM SIGMOD International Conference on Management of data*. 339–350.
- [23] Andreas Kipf, Thomas Kipf, Bernhard Radke, Viktor Leis, Peter Boncz, and Alfons Kemper. 2018. Learned cardinalities: Estimating correlated joins with deep learning. *arXiv preprint arXiv:1809.00677* (2018).
- [24] Andreas Kipf, Ryan Marcus, Alexander van Renen, Mihail Stoian, Alfons Kemper, Tim Kraska, and Thomas Neumann. 2019. SOSD: A Benchmark for Learned Indexes. *NeurIPS Workshop on Machine Learning for Systems* (2019).
- [25] Andreas Kipf, Ryan Marcus, Alexander van Renen, Mihail Stoian, Alfons Kemper, Tim Kraska, and Thomas Neumann. 2020. RadixSpline: a single-pass learned index. In *Proceedings of the Third International Workshop on Exploiting Artificial Intelligence Techniques for Data Management, aiDM@SIGMOD 2020, Portland, Oregon, USA, June 19, 2020*. 5:1–5:5. <https://doi.org/10.1145/3401071.3401659>
- [26] Tim Kraska, Mohammad Alizadeh, Alex Beutel, Ed H Chi, Jialin Ding, Ani Kristo, Guillaume Leclerc, Samuel Madden, Hongzi Mao, and Vikram Nathan. 2019. Sagedb: A learned database system. (2019).
- [27] Tim Kraska, Alex Beutel, Ed H Chi, Jeffrey Dean, and Neoklis Polyzotis. 2018. The case for learned index structures. In *Proceedings of the 2018 International Conference on Management of Data*. 489–504.
- [28] Tim Kraska, Umar Farooq Minhas, Thomas Neumann, Olga Papaemmanouil, Jignesh M Patel, Chris Ré, and Michael Stonebraker. 2021. ML-In-Databases: Assessment and Prognosis. *IEEE Data Engineering Bulletin* 44, 1 (2021), 3.
- [29] Sanjay Krishnan, Zongheng Yang, Ken Goldberg, Joseph Hellerstein, and Ion Stoica. 2018. Learning to optimize join queries with deep reinforcement learning. *arXiv preprint arXiv:1808.03196* (2018).
- [30] Martijn HR Lankhorst, Bas WSMM Ketelaars, and Robertus AM Wolters. 2005. Low-cost and nanoscale non-volatile memory concept for future silicon chips. *Nature materials* 4, 4 (2005), 347–352.
- [31] Tobin J Lehman and Michael J Carey. 1985. *A study of index structures for main memory database management systems*. Technical Report. University of Wisconsin-Madison Department of Computer Sciences.
- [32] Viktor Leis, Alfons Kemper, and Thomas Neumann. 2013. The adaptive radix tree: ARTful indexing for main-memory databases. In *2013 IEEE 29th International Conference on Data Engineering (ICDE)*. IEEE, 38–49.
- [33] Pengfei Li, Hua Lu, Qian Zheng, Long Yang, and Gang Pan. 2020. LISA: A learned index structure for spatial data. In *Proceedings of the 2020 ACM SIGMOD International Conference on Management of Data*. 2119–2133.

- [34] Lin Ma, Bailu Ding, Sudipto Das, and Adith Swaminathan. 2020. Active learning for ML enhanced database systems. In *Proceedings of the 2020 ACM SIGMOD International Conference on Management of Data*. 175–191.
- [35] Yandong Mao, Eddie Kohler, and Robert Tappan Morris. 2012. Cache craftiness for fast multicore key-value storage. In *Proceedings of the 7th ACM european conference on Computer Systems*. 183–196.
- [36] Ryan Marcus, Andreas Kipf, Alexander van Renen, Mihail Stoian, Sanchit Misra, Alfons Kemper, Thomas Neumann, and Tim Kraska. 2020. Benchmarking Learned Indexes. *Proc. VLDB Endow.* 14, 1 (2020), 1–13.
- [37] Ryan Marcus and Olga Papaemmanouil. 2018. Towards a hands-free query optimizer through deep learning. *arXiv preprint arXiv:1809.10212* (2018).
- [38] Ryan Marcus, Emily Zhang, and Tim Kraska. 2020. Cdfshop: Exploring and optimizing learned index structures. In *Proceedings of the 2020 ACM SIGMOD International Conference on Management of Data*. 2789–2792.
- [39] Michael Mitzenmacher. 2018. A model for learned bloom filters and related structures. *arXiv preprint arXiv:1802.00884* (2018).
- [40] C Mohan. 1989. *ARIES/KVL: A key-value locking method for concurrency control of multiaction transactions operating on B-tree indexes*. IBM Thomas J. Watson Research Division.
- [41] Vikram Nathan, Jialin Ding, Mohammad Alizadeh, and Tim Kraska. 2020. Learning multi-dimensional indexes. In *Proceedings of the 2020 ACM SIGMOD International Conference on Management of Data*. 985–1000.
- [42] Jennifer Ortiz, Magdalena Balazinska, Johannes Gehrke, and S Sathya Keerthi. 2018. Learning state representations for query optimization with deep reinforcement learning. In *Proceedings of the Second Workshop on Data Management for End-To-End Machine Learning*. 1–4.
- [43] Varun Pandey, Alexander van Renen, Andreas Kipf, Ibrahim Sabek, Jialin Ding, and Alfons Kemper. 2020. The case for learned spatial indexes. *arXiv preprint arXiv:2008.10349* (2020).
- [44] Yongjoo Park, Ahmad Shahab Tajik, Michael Cafarella, and Barzan Mozafari. 2017. Database learning: Toward a database that becomes smarter every time. In *Proceedings of the 2017 ACM International Conference on Management of Data*. 587–602.
- [45] Jianzhong Qi, Guanli Liu, Christian S Jensen, and Lars Kulik. 2020. Effectively learning spatial indices. *Proceedings of the VLDB Endowment* 13, 12 (2020), 2341–2354.
- [46] Jun Rao and Kenneth A. Ross. 1999. Cache Conscious Indexing for Decision-Support in Main Memory. In *Proceedings of the 25th International Conference on Very Large Data Bases (VLDB '99)*. Morgan Kaufmann Publishers Inc., San Francisco, CA, USA, 78–89.
- [47] Jun Rao and Kenneth A Ross. 2000. Making B+-trees cache conscious in main memory. In *Proceedings of the 2000 ACM SIGMOD international conference on Management of data*. 475–486.
- [48] Venkathachary Srinivasan and Michael J Carey. 1991. Performance of B-tree concurrency control algorithms. In *Proceedings of the 1991 ACM SIGMOD international conference on Management of data*. 416–425.
- [49] Mihail Stoian, Andreas Kipf, Ryan Marcus, and Tim Kraska. 2021. PLEX: Towards Practical Learned Indexing. *arXiv preprint arXiv:2108.05117* (2021).
- [50] Ji Sun, Guoliang Li, and Nan Tang. 2021. Learned Cardinality Estimation for Similarity Queries. In *Proceedings of the 2021 International Conference on Management of Data*. 1745–1757.
- [51] Peter Van Sandt, Yannis Chronis, and Jignesh M Patel. 2019. Efficiently Searching In-Memory Sorted Arrays: Revenge of the Interpolation Search?. In *Proceedings of the 2019 International Conference on Management of Data*. 36–53.
- [52] Haixin Wang, Xiaoyi Fu, Jianliang Xu, and Hua Lu. 2019. Learned index for spatial queries. In *2019 20th IEEE International Conference on Mobile Data Management (MDM)*. IEEE, 569–574.
- [53] Jiacheng Wu, Yong Zhang, and Shimin Chen. 2021. Updatable Learned Index with Precise Positions. *Proceedings of the VLDB Endowment* 14, 8 (2021), 1276–1288.
- [54] Peizhi Wu and Gao Cong. 2021. A Unified Deep Model of Learning from both Data and Queries for Cardinality Estimation. In *Proceedings of the 2021 International Conference on Management of Data*. 2009–2022.
- [55] Huanchen Zhang, David G Andersen, Andrew Pavlo, Michael Kaminsky, Lin Ma, and Rui Shen. 2016. Reducing the storage overhead of main-memory OLTP databases with hybrid indexes. In *Proceedings of the 2016 International Conference on Management of Data*. 1567–1581.

A DETAILS OF INNER NODES

A.1 Linear Regression Node

Linear regression node (LR node) is the type of inner node that uses linear regression to determine the next branch. As mentioned in Section 5.1, the size of tree nodes must be 64 bytes. We only use a simple linear model in this node to achieve the goal of predicting the position as quickly as possible, and the remaining bytes are

placeholders. For a given input key, the next branch can be directly obtained by a few simple calculations and boundary processing. Figure 16 shows the memory layout and detailed computation steps of LR nodes for reference.

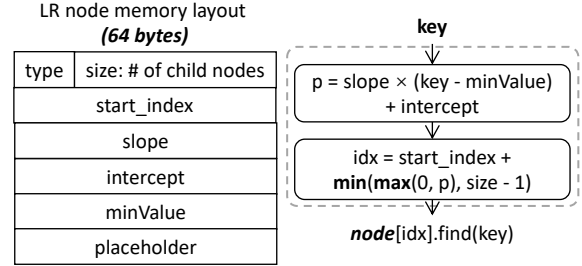


Figure 16: Details of LR Node

A.2 Piecewise Linear Regression Node

Piecewise linear regression node (P. LR node) uses a piecewise linear regression model to determine the next branch. More specifically, the piecewise linear model contains $kIndexNum + 1$ segments, and we store the coordinates of the segment end points in the P. LR node. Due to the fixed number of segments, the training method of the PLR node, which is related to the segment point, is slightly different from the least-squares method of the LR node. $kIndexNum$ is calculated from the size of the key type to ensure that the total size does not exceed 64 bytes, and placeholders fill the part less than 64 bytes. For a 32-bit key, its value is 6, which means that there are a total of 8 linear models. When we traverse through a P. LR node, we first find the segment to which the input key belongs, then use the segment as a linear model to determine the next branch. The memory layout and internal mechanism of a P. LR node are demonstrated in Figure 17.

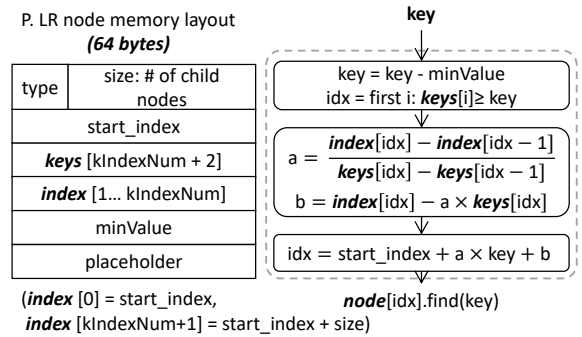


Figure 17: Details of P. LR Node

A.3 Binary Search Node

Binary search node (BS node) uses a binary search procedure to determine the corresponding branch for the input key value. This is very similar to traversing through B+ Tree, the only difference is that the reference table in a BS node is determined during the index construction procedure, and remains fixed afterward.

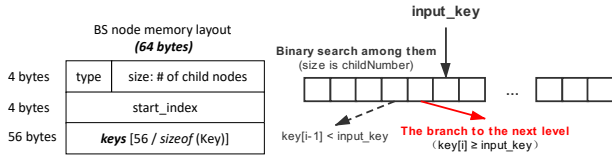


Figure 18: Details of BS Node

Each BS node stores $\frac{56}{\text{sizeof}(key)}$ key values internally, and divides the key range into $\frac{56}{\text{sizeof}(key)} + 1$ intervals. To determine which branch to go through, a binary search is performed among the stored key values to locate the corresponding key value interval covering the input key. Figure 18 shows the details of the BS nodes.

A.4 Histogram Node

Histogram nodes find the corresponding branch directly through a simple one-step calculation and table look-up operation.

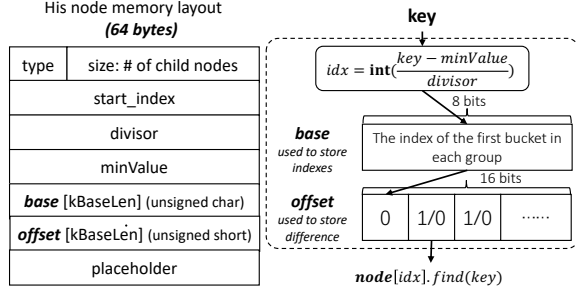


Figure 19: Details of Hist Node

The look-up table in Histogram node is stored very compactly using two tables. Each byte in *Base* represents the index in child nodes of the first bit of the corresponding 16 bits in *Offset*. Each bit of *Offset* represents the difference (0 or 1) between the index of the current bucket and the previous bucket, as shown in Figure 19. To determine the next branch, we only need to visit *Base* to get the base index, and then count the number of bits in the *Offset* table, and finally add them together to get the index of the next branch.

B DETAILS OF LEAF NODES

B.1 CF Array Leaf Node

In cache-friendly array leaf nodes (CF node), the data points are compactly stored in data blocks in a sequential manner. When searching for data points in the CF array leaf nodes, we first search sequentially in the keywords of each block, and then search in the block. When we need to insert a given data point, we must first find the correct position, and then move all the data points by one cell to make room for the new data point. The memory layout and internal mechanism of a CF leaf node are demonstrated in Figure 20.

B.1.1 Insert Operation. In Section 5.2.2, we have introduced the procedure of insert operations with two general mechanisms to make room for the data points to be inserted. In the implementation

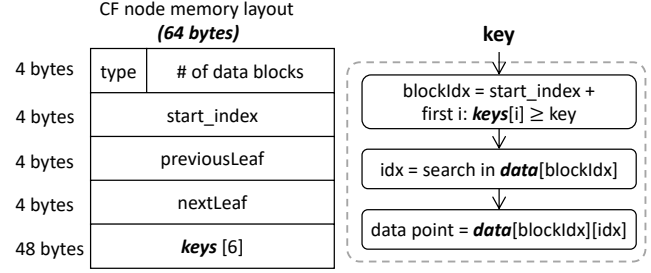


Figure 20: Details of CF Nodes

of CARMi, we actually use three mechanisms in the CF leaf node: rebalance, expand, and split. Figure 21 shows the mechanisms of them. Here we explain the rebalance mechanism that has not been introduced.

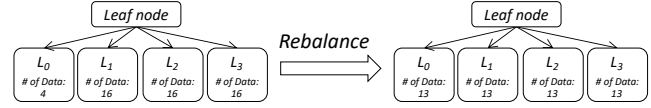


Figure 21: Rebalance Mechanism

When the data block to be inserted is full, but the next data block is not full, we will insert the data point into the next block. In order to keep all data points managed by this leaf node in order, the inserted data point will be compared with the largest one in the current block. The larger one is inserted into the next block, and the other is stored in the current block. If the next data block is also saturated, the rebalance mechanism is triggered. The leaf node collects all data points in its data blocks and reallocates them evenly to all these blocks. This mechanism can make the data distribution in data blocks more even, reducing a certain amount of time for subsequent insert.

B.2 External Array Leaf Node

The external array leaf node uses a simple linear model to predict the location, and the pointer no longer points to the data array but to the external location. The external array leaf node is used to create an index over a sorted array of data points (e.g., primary indexes in databases), and we use this type of node to create an index for the YCSB dataset. Its access flow is shown in Figure 22.

Inevitably, the accuracy of the model prediction cannot reach 100%, so we need a subsequent binary search step to find the exact position of the data record. For this purpose, we employ an additional parameter: the error ϵ , whose value is determined during the training process. For a given key value x , let us denote the actual location of the data point as $loc(x)$, and the predicted location of the data point as $preIdx(x)$. Then, when looking for the data point matching x , depending on the relationship between these two terms, there are essentially two cases: either $loc(x) \in [preIdx(x) - \frac{\epsilon}{2}, preIdx(x) + \frac{\epsilon}{2}]$, or $loc(x)$ is outside of this range. The time cost of data access is also different for these two cases. In the former case, we need to perform a binary search over the range of $[preIdx(x) - \frac{\epsilon}{2}, preIdx(x) + \frac{\epsilon}{2}]$, while in the latter case the range of the binary search is the entire array.

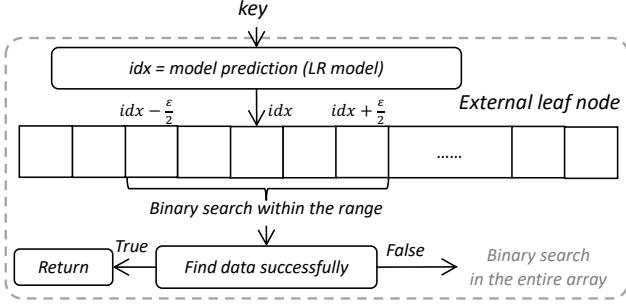


Figure 22: Details of External Array Leaf Nodes

B.2.1 The Optimal Value of Error Parameters. Essentially, we want to choose the error parameter ϵ that minimizes the average time cost of data access. The method for finding its optimal value is given below. Let us denote for each data point its true position as y_i , the predicted value as p_i , and their difference $d_i = y_i - p_i$. With these notations, we can compute the average time cost of data access as in Equation (10).

$$Avg = \frac{1}{n} [|\{i : |d_i| \leq \frac{\epsilon}{2}\}| \cdot [\log_2 \epsilon] + |\{i : |d_i| > \frac{\epsilon}{2}\}| \cdot [\log_2 n]] \quad (10)$$

Then, we only need to substitute different ϵ values into Equation (10) to find the minimum value of Avg , where the range of ϵ is from 0 to $\max |p_i - y_i|$.

$$\epsilon = \arg \min_{\epsilon} [|\{i : |d_i| \leq \frac{\epsilon}{2}\}| \cdot [\log_2 \epsilon] + |\{i : |d_i| > \frac{\epsilon}{2}\}| \cdot [\log_2 n]]$$

C DETAILS OF ROOT NODES

C.1 Linear Regression Root Node

The linear regression root node is a very simple root node consisting of a linear regression model. In addition to the basic members, only two linear model parameters need to be stored. We only need one model prediction and the boundary condition processing to get the index of the next node. The details of LR root node is shown in Figure 23.

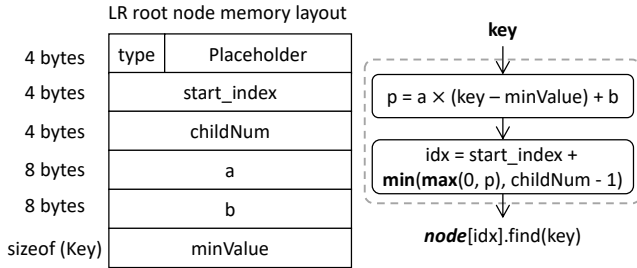


Figure 23: Details of LR Root Nodes

C.2 Piecewise Linear Regression Root Node

The P. LR root node uses a piecewise linear regression model with up to five segments to allocate the dataset to the child nodes. It differs from the P. LR inner nodes only in the number of segments. We use a dynamic programming algorithm similar to the prefetch

model to find the optimal segmentation points and the number of segments, thereby maximizing the entropy of the node. Since the root node is in the cache, we do not limit its size here. For the P. LR root node, we find the first breakpoint greater than or equal to the key value, and then use the corresponding model parameters for calculation and boundary processing, as shown in Figure 24.

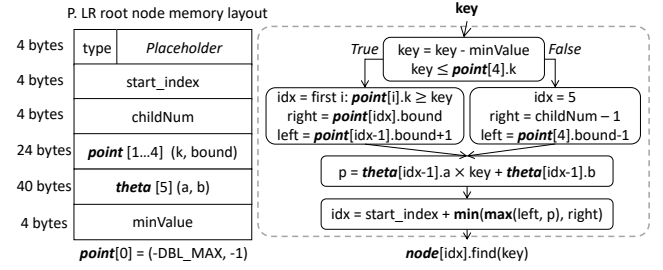


Figure 24: Details of P. LR Root Nodes

D PARAMETER SETTINGS

This section describes the default parameter settings in our experiments. The default value of the parameter λ used to tradeoff between the time cost and space cost is 0.03, but we adjusted this parameter in the experiments according to the datasets and the needs of the experiments. The size of each data block is represented as $kBlockSize$, and the default value is 256 bytes, and the maximum capacity of external leaf nodes is 512. The parameter $kDPTThreshold$ is used to switch between the dp and greedy algorithms and its value is 512. When a leaf node needs to perform a split operation, we need to replace it with an inner node and $kDividedNodeNum$ leaf nodes with a default value of 16. The parameter $kLeafThreshold$ is 90, which means that when the number of data points is less than 90, the algorithm will directly construct a leaf node instead of choosing a better one from leaf nodes and inner nodes, thus saving a certain amount of space cost and construction time. Note that this parameter must be smaller than $kLeafMaxCapacity$. Table 9 lists these parameters with default values for a quick view.

E PROOF OF THEOREM 3.1

PROOF. W.l.o.g, let M_1, \dots, M_I be the set of inner nodes, and M_{I+1}, \dots, M_K be the set of leaf nodes. Let n_i be the number of data points in node M_i , and C_i be the set of child nodes of M_i . Then, we can substitute the definition of $P(M_i)$ and $H(M_i)$ into Theorem 3.1:

$$\begin{aligned} \sum_{i=1}^K P(M_i)H(M_i) &= - \sum_{i=1}^I \frac{n_i}{n} \sum_{j \in C_i} \frac{n_j}{n_i} \log_2 \frac{n_j}{n_i} + \sum_{i=I+1}^K \frac{n_i}{n} \log_2 n_i \\ &= - \sum_{i=1}^I \sum_{j \in C_i} \frac{n_j}{n} \log_2 \frac{n_j}{n_i} + \sum_{i=I+1}^K \frac{n_i}{n} \log_2 n_i \end{aligned}$$

For each leaf node M_I , let the traverse path from the root to M_I be $Root \rightarrow M_{i_1} \rightarrow M_{i_2} \rightarrow \dots \rightarrow M_{i_k} \rightarrow M_I$. We can define P_i as the following set: $P_i = \{(Root, M_{i_1}), (M_{i_1}, M_{i_2}), \dots, (M_{i_k}, M_I)\}$. Then, the double summation can be rearranged according to all the

Table 9: The Settings of Parameters

Params	Explanation	Default Value
λ	several different values were used in experiments	0.03
$kBlockSize$	the fixed size of a data block	256
$kLeafMaxCapacity$	(1) the maximum capacity of CF nodes (2) the maximum capacity of external nodes	96 512
$kDPThreshold$	used to switch between DP and greedy algorithms	512
$kDividedNodeNum$	the number of new leaf nodes in split mechanism	16
$kLeafThreshold$	the size threshold in DP transition	90

paths from the root node to the leaf nodes:

$$-\sum_{i=1}^I \sum_{j \in C_i} \frac{n_j}{n} \log_2 \frac{n_j}{n_i} = \sum_{i=1}^I \sum_{j \in C_i} \sum_{l: (M_i, M_j) \in P_l} \frac{n_l}{n} \log_2 \frac{n_i}{n_j}$$

where we split $\frac{n_j}{n}$ according to whether the l -th leaf node is visited to obtain $\sum_{l: (M_i, M_j) \in P_l} \frac{n_l}{n}$.

Then we sort and rearrange them according to each path to the leaf node:

$$-\sum_{i=1}^I \sum_{j \in C_i} \frac{n_j}{n} \log_2 \frac{n_j}{n_i} = \sum_{l=I+1}^K \frac{n_l}{n} \sum_{(M_i, M_j) \in P_l} \log_2 \frac{n_i}{n_j}$$

Finally, we merge the above equation with the leaf node part

$$\sum_{i=1}^K P(M_i)H(M_i) = \sum_{l=I+1}^K \frac{n_l}{n} \left(\sum_{(M_i, M_j) \in P_l} \log_2 \frac{n_i}{n_j} + \log_2 n_l \right)$$

and simplify the equation in the path order:

$$\begin{aligned} \sum_{i=1}^K P(M_i)H(M_i) &= \sum_{l=I+1}^K \frac{n_l}{n} (\log_2 \frac{n}{n_l} + \log_2 n_l) \\ &= \sum_{l=I+1}^K \frac{n_l}{n} \log_2 n \\ &= \log_2 n \end{aligned}$$

where $\sum_{l=I+1}^K n_l$ is equal to n . □